

Loss rate of ultracold neutrons due to the absorption by trap walls in large material traps

Pavel D. Grigoriev,^{1,2,3,*} Vladislav D. Kochev,^{2,4,1} Victor A. Tsyplukhin,² Alexander M. Dyugaev,¹ and Ilya Ya. Polishchuk^{4,5}

¹*L. D. Landau Institute for Theoretical Physics, 142432, Chernogolovka, Russia*

²*Theoretical Physics and Quantum Technologies Department,*

National University of Science and Technology "MISIS", 119049, Moscow, Russia

³*National Research University Higher School of Economics, Moscow, 101000, Russia*

⁴*NRC Kurchatov Institute, 123182, Moscow, Russia*

⁵*Theoretical Physics Department, Moscow Institute For Physics and Technology, 141700, Dolgoprudnii, Russia*

(Dated: December 18, 2024)

The most accurate neutron lifetime measurements now use the material or magnetic traps of ultracold neutrons (UCN). The precision of these experiments is determined by the accuracy of estimating the neutron loss rate. In material UCN traps the main source of neutron losses is the absorption by trap walls. In this paper we analyze the standard methods and their approximations for the calculation of UCN absorption rate by the walls of material traps. We emphasize the approximations used both in the standard analytical formulas and in the numerical Monte-Carlo simulations. For the two simplest trap geometries, rectangular and cylindrical, we obtain analytical formulas for this absorption rate provided the UCN velocity distribution is isotropic at trap bottom. Then we perform numerical calculations of UCN velocity distribution and absorption rate taking into account the diffuse elastic UCN reflections by trap walls obeying two different laws: Lambert's cosine law and isotropic reflection. We compare the results with the standard estimation methods and discuss the differences. We indicate the difference between the UCN *number* and *density* velocity distribution. Our results may be useful to resolve the puzzling four-second discrepancy between the magnetic and material-trap measurements of neutron lifetime.

I. INTRODUCTION

The neutron β -decay $n \rightarrow p + e^- + \bar{\nu}_e$ plays an important role in cosmology, astrophysics and elementary particle physics (see [1–7] for reviews). The primordial light element abundance is very sensitive to the exact value of neutron mean lifetime τ_n [1, 8]. The precise τ_n -measurements, combined with decay correlations in polarized-neutron decay experiments [9–12], test the standard model and give the coupling constants of the weak interaction [1–4, 9–13]. The measurements of neutron electric dipole moment (EDM) [14–17] impose the upper limits on CP violation. The resonant transitions between discrete quantum energy levels of neutrons in the earth gravitational field [18–20] probe the gravitational field on a micron length scale and impose constraints on dark matter.

These and other neutron experiments mostly employ the ultracold neutrons (UCN) with energy E lower than either the neutron optical potential of typical materials or the Zeeman energy of neutron spin in available magnetic fields, i.e. $E \lesssim 300$ neV [11, 12, 14–36]. In material traps UCN can be trapped for many minutes in specially designed "neutron bottles" [24–30], where the earth gravitational field 100 neV per meter plays an important role in UCN storage and manipulation [21–28]. The Fomblin grease is currently used to cover the UCN trap walls [24–30] in the bottle UCN experiments and allows reaching the very high accuracy of neutron lifetime measurements in large gravitational traps [27]: $\tau_n = 881.5 \pm 0.7$ (stat) ± 0.6 (syst) s. The neutron magnetic moment of 60 neV/T allows magneto-gravitational trapping of UCN [31–36], giving even higher claimed accuracy of latest UCN- τ measurements [36]: $\tau_n \approx 877.7 \pm 0.28$ (stat) $^{+0.22}_{-0.16}$ (syst) s. The neutron lifetime

measured using magnetic traps [36] is about 4 seconds smaller than in the UCN material-bottle experiments [27], which is beyond the 3σ deviation.

The most precise time-of-flight τ_n -measurements with the beam of cold neutrons give $\tau_n = 887.7 \pm 1.2$ (stat) ± 1.9 (syst) s [37–39], which is about 10 seconds greater than in the UCN magnetic traps. The large discrepancy between τ_n measured using the beam and UCN material- or magnetic-trap methods is called the "neutron lifetime puzzle" and receives extensive discussion till now [39–43]. Presumably, this is due to systematic errors in beam experiments [41], but unaccounted UCN losses in the bottle material and magnetic trap τ_n measurements have not yet been excluded. The analysis of neutron β -decay asymmetry [44] suggests that this discrepancy is unlikely caused by new physics, for example, by dark matter and additional neutron decay channels or excited states [39, 40].

The precision of τ_n measurements using UCN traps, both material and magnetic, is determined by the accuracy of estimating the neutron loss rate from the traps, which is the main source of systematic errors [21–28, 34–36, 45]. The main UCN loss mechanism from magnetic traps, as listed in Table II of Ref. [36], include (i) UCN spin depolarization, for example, because of the nonuniform magnetic field and, hence, its nonzero perpendicular-to-spin component; (ii) heated UCNs; (iii) residual gas scattering; (iv) uncleaned higher-energy UCNs. In this paper we do not discuss the accuracy of magnetic-trap UCN experiments and consider only the material traps.

The material UCN traps are, usually, coated with Fomblin grease, providing the highest accuracy of τ_n measurements. The Fomblin grease has the optical potential barrier $V_0^F \approx 106$ neV. The probability of neutron absorption by such a wall is $\sim 10^{-5}$ per collision [6, 21–23]. In addition, the inelastic UCN scattering by trap walls, when the neutron absorbs a thermal excitation, increases the UCN energy above the potential

* Corresponding author, e-mail: grigorev@itp.ac.ru

barrier V_0 and also leads to neutron losses. Therefore, the neutron lifetime τ_n is estimated by the double extrapolation of the measured lifetime $\tau_m < \tau_n$ of UCN stored in the trap to zero temperature (thermal extrapolation) and to an infinite trap size (geometrical or size extrapolation). The extrapolation interval is rather large, usually, $\tau_n - \tau_m \gtrsim 20$ s. This limits the precision of τ_n measurements in material traps, because the estimate of UCN loss rate with an accuracy better than 5% is very complicated.

The UCN absorption probability depends on the angle of incidence during each collision and, hence, on UCN height and angular velocity distribution. The usually applied assumption [27] of the uniform distribution of neutron velocity direction with respect to the trap surface at any height may be violated because the vertical UCN velocity component of each neutron during its motion depends on the height above trap bottom due to gravity. This difficulty can be overcome by Monte-Carlo simulations [46–51] of UCN losses taking into account the calculated incidence angles of each collision for the particular trap geometry, provided the initial momentum distribution of UCN is known and the applied simple physical model of UCN interaction with trap walls is correct. The Monte-Carlo simulations are also actively used to estimate the UCN losses in magnetic traps [52]. A more serious problem is the surface roughness of material traps, which makes impossible the exact calculation of UCN scattering angle and loss probability during each collision.

The UCN losses on trap walls and the extrapolation interval can be reduced by increasing the trap size and, hence, the volume-to-surface ratio in material traps. However, even with a very large UCN trap with size 2 m in the recent τ_n measurements [27] the extrapolation interval $\tau_n - \tau_m$ was only reduced to 20 seconds. A further size increase of UCN traps is not only technically problematic but also not very useful, because the main UCN losses already come from their collisions with the trap bottom, and the rate of these collisions is determined by the Earth gravity and by the UCN kinetic energy $E_k < V_0$, rather than by the trap size.

A possible qualitative way to reduce the UCN absorption rate is to cover the trap walls by liquid ^4He , the only material that does not absorb neutrons [53–59]. However, covering the UCN trap walls by liquid helium has several drawbacks. First, ^4He creates a very small optical potential barrier $V_0^{\text{He}} = 18.5$ neV for neutrons, which is 5.7 times smaller than the barrier height $V_0^{\text{F}} \approx 106$ neV of Fomblin oil. Hence, the UCN phase volume and their density in such a trap is reduced by the factor $(V_0^{\text{F}}/V_0^{\text{He}})^{3/2} \approx 13.7$ as compared to the Fomblin coating, which enhances the statistical errors. The UCN production technology develops [7, 60, 61], and this reduction of neutron density may become less important than the advantage of decreasing the UCN absorption rate. The second problem with the liquid ^4He coating of UCN trap walls is that a very low temperature $T < 0.5$ K is required. At higher T the concentration of ^4He vapor is rather high, leading to the inelastic UCN scattering with large energy transfer $\sim k_B T \gg V_0^{\text{He}}$ from the vapor atoms to neutrons. The third problem with liquid ^4He is another source of inelastic UCN scattering – the thermally activated quanta of surface waves, called ripplons.

They lead to a linear temperature dependence of scattering rate [56], surviving even at ultra-low temperature. The strength of neutron-ripplon interaction is rather small [56], which makes feasible the UCN storage in He-covered traps, and the linear temperature dependence of UCN losses due to their scattering by ripplons is very convenient for taking into account this systematic error. However, the UCN scattering by ripplons strongly limits the possible advantage of using liquid helium in the UCN storage. Hence, below we consider more traditional and currently used UCN traps, where the wall material absorbs neutrons.

The "neutron lifetime puzzle", i.e. the difference between τ_n -measurements using cold neutron beam and material UCN traps, is generally attributed to the errors in beam experiments [41]. However, the 4-second discrepancy between the results of latest magnetic-trap and material-bottle τ_n measurements remains puzzling. Notably, the former also very precise measurements of UCN lifetime using a material trap gave the value [24] $\tau_n = 878.5 \pm 0.7$ (stat) ± 0.3 (sys) s, which is 3 seconds smaller than the result of Ref. [27] and much closer to the magnetic-trap τ_n measurements. The difference between Refs. [27] and [24] is not only a larger size but also the different shape of UCN trap used in the experiment [27]. As we show below, the size extrapolation used to estimate the UCN loss rate τ_{loss}^{-1} due to the absorption by trap walls is rather sensitive to the trap shape, which may give a 3-second difference to the measured τ_n . In this paper we reanalyze the estimate method of UCN loss rate τ_{loss}^{-1} from the absorption by trap walls and consider several important assumptions which may lead to errors in the extracted value of neutron lifetime.

In Sec. II we summarize the standard estimate procedures of UCN loss rate in material traps and emphasize their approximations. In Sec. III we analytically calculate the UCN absorption rate for two simple trap shapes, assuming the uniform and isotropic velocity distribution of UCN at trap bottom, and show the difference between various estimate methods of UCN loss-rate calculations. In Sec. IV we performed Monte-Carlo simulations of UCN distribution and absorption by trap walls. In Sec. V we discuss the results and their consequences on the size scaling and on the accuracy of estimates of neutron loss rate and lifetime.

II. STANDARD ESTIMATE PROCEDURE OF NEUTRON LOSSES IN UCN TRAPS AND ITS DISCUSSION

A. Basic formulas

The methods of estimating τ_{loss}^{-1} start from the well-known formula [21–23] for the absorption probability of neutron by the wall during each scattering

$$\mu(v_{\perp}) = \frac{2\eta v_{\perp}/v_{\text{lim}}}{\sqrt{1 - (v_{\perp}/v_{\text{lim}})^2}}, \quad (1)$$

where η is the loss coefficient depending on the wall material, v_{\perp} is the normal-to-wall UCN velocity, and to the v_{lim} is the limiting velocity, corresponding to the UCN kinetic energy E_k

equal to the potential barrier $V_0 = m_n v_{\text{lim}}^2 / 2$, created by trap material. Then one usually assumes a uniform distribution of the incidence angle of UCN on the walls. The integration of Eq. (1) over the solid incidence angle gives another well-known formula [21–23] for the averaged absorption probability

$$\bar{\mu}(v_*) = \frac{2\eta}{v_*^2} \left(\arcsin v_* - v_* \sqrt{1 - v_*^2} \right) \approx \begin{cases} \pi\eta, & v_* \rightarrow 1 \\ 4\eta v_*/3, & v_* \ll 1 \end{cases}, \quad (2)$$

where the normalized velocity $v_* \equiv v/v_{\text{lim}} = \sqrt{E_k/V_0}$. We rewrite Eq. (2) as

$$\bar{\mu}(E_*) = 2\eta f_1(E_*), \quad (3)$$

introducing the normalized UCN energy $E_* \equiv E_k/V_0 = v_*^2$ and the dimensionless function

$$f_1(x) = \frac{1}{x} \left(\arcsin \sqrt{x} - \sqrt{x} \sqrt{1-x} \right), \quad (4)$$

which describes the effective collision rate of UCN with trap walls.

B. Gravity effects and size extrapolation

The averaged absorption probability $\bar{\mu}$ depends on UCN kinetic energy E_k , which due to the Earth gravity depends on the height h above the trap bottom as $E_k(h) = E - m_n g h = E - h'$, where E is total UCN energy, equal to the kinetic neutron energy at the trap bottom $h = 0$, g is the free-fall acceleration, and $h' \equiv m_n g h$. The corresponding height dependence of neutron velocity $v_*(h) = \sqrt{(E - m_n g h)/V_0}$ is, usually, taken into account by the integration of the averaged scattering rate $\bar{\mu}(E_k)$ over the trap surface as [24, 27]

$$\tau_{(g)}^{-1}(E) = \frac{\int_0^{h_{\text{max}}(E)} dS(h) \bar{\mu}(E - h') v(E - h') \rho(E, h')}{4 \int_0^{h_{\text{max}}(E)} dV(h) \rho(E, h')} \equiv \eta \gamma(E), \quad (5)$$

where according to Ref. [27] the UCN number density

$$\rho(E, h) \propto \sqrt{(E - h')/E} \quad (6)$$

gives the energy and height distribution of UCN in the trap,

$$h_{\text{max}}(E) \equiv E/m_n g = v^2/2g \equiv h_{\text{lim}} E_* \quad (7)$$

is the maximal height of neutrons with energy E , and $\gamma(E)$ is the effective collision frequency of UCN with the walls. This effective UCN collision frequency also enters the size extrapolation formula that gives the neutron β -decay time τ_n from two measured lifetimes τ_1 and τ_2 in two UCN traps of different size [27]:

$$\tau_n^{-1} = \tau_1^{-1} - \left(\tau_2^{-1} - \tau_1^{-1} \right) \left/ \left(\frac{\gamma_2(E)}{\gamma_1(E)} - 1 \right) \right. . \quad (8)$$

For the traps of height $h \ll h_{\text{lim}}$ one can simplify further, ignoring the gravity effects and assuming the isotropic velocity

distribution. The ratio of effective collision frequencies is then taken as the ratio of surface-to-volume ratios of two different traps [22]:

$$\frac{\gamma_2(E)}{\gamma_1(E)} = \frac{S_2}{V_2} \bigg/ \frac{S_1}{V_1}. \quad (9)$$

According to Eq. (9), one obtains the following simple formula for the UCN loss rate

$$\tau_{(s)}^{-1}(E) = \frac{\bar{\mu}(E) v(E) S}{4V}. \quad (10)$$

Below we compare these two results, given by Eqs. (5) and (10), with another estimations for several simple trap shapes.

C. Problems with standard size extrapolation and with estimates of UCN losses

Evidently, Eq. (9) is oversimplified and contradicts Eq. (5), because the two UCN traps are, usually, not geometrically similar. Even if they are similar in shape and differ only in size, the gravity effects violate the simple formula (9). Therefore, in Refs. [24, 27] Eq. (5) was used to estimate $\gamma(E)$. However, the energy dependence of $\tau_{(g)}^{-1}(E)$ and $\gamma(E)$ in Eq. (5) makes the size extrapolation to be energy dependent too. This problem can be partially solved by the integration of the result for $\tau_{(g)}^{-1}(E)$ over energy with the actual energy distribution $n(E)$ of UCN. Then the final τ_n result (8) depends on the distribution function $n(E)$. This function is unknown. In Ref. [27] it was initially assumed Maxwellian and then corrected by fitting the energy spectrum of UCN reaching the detector, which can be measured. However, even this fitting procedure does not ensure that the distribution function $n(E)$ is found precisely.

Another important problem is that Eqs. (3) and (5) are also approximate, because the gravity changes not only the neutron energy, as described by Eq. (5), but also the velocity distribution, because it affects only the vertical z -component of UCN velocity. Hence, the assumption of uniform angular distribution of UCN velocities, implied in Eqs (3) and (5), even if holds at the trap bottom, may violate on the side trap walls at $h \neq 0$. If this anisotropy of velocity distribution appears, it can be compensated by a proper choice of the function $\bar{\mu}^*(y)$, which then depends on the trap size and geometry. By the Monte-Carlo simulations it was shown [27] that while the result of energy extrapolation is very sensitive to the function $\bar{\mu}(y)$ and differs by 40 seconds for different $\bar{\mu}(y)$, the result of subsequent size extrapolation is much less sensitive to the function $\bar{\mu}(y)$ and varies within the interval of only 4 seconds. Another important issue to be considered is the proper dependence of the collision rate on UCN velocity. Even if the UCN velocity distribution is isotropic, for each neutron the dependence of collision rate on its vertical velocity strongly differs from that for horizontal, as follows from Eq. (12) below. Then the effective collision rate is not given by Eqs. (2)-(4), which affects the accuracy of UCN loss estimates. Of course, the diffuse UCN scattering by trap walls complicates the above arguments. But can it restore the validity of Eq. (5)?

There is also a more fundamental question about the validity of Eq. (1) for the neutron absorption rate during the collisions, especially for the walls with imperfections as pores or rough unflat surface. This problem can be partially solved covering the trap wall by a liquid film, as ^4He in the proposal of Refs. [53–59]. However, the typical experiments are performed at higher temperature and with solid trap walls, e.g. the Fomblin grease [24–30]. In this paper we assume Eq. (1) to be valid, and for several simple UCN trap shapes we analyze the effect of the above mentioned anisotropy of UCN velocity distribution and of effective collision frequency on the UCN loss rate and on the accuracy of τ_n extraction.

III. ANALYTICAL FORMULAS FOR UCN LOSSES IN RECTANGULAR AND CYLINDRICAL TRAPS

A. General formulas

For a rectangular UCN trap of size $L_x \times L_y \times L_z$ the neutron motion along three main axes separate, because any elastic scattering by the trap wall perpendicular to axis i only changes the sign of neutron velocity v_i along this axis. The absorption probability during each collision is given by Eq. (1) and also depends only on the same velocity component $v_i = v_\perp$:

$$\mu_i(v_i) = \frac{2\eta v_i/v_{\text{lim}}}{\sqrt{1 - v_i^2/v_{\text{lim}}^2}}. \quad (11)$$

The number of collisions with the walls during a long time $t \gg L_i/v_i$ for each neutron can be easily estimated:

$$\mathcal{N}_x = \frac{tv_x}{L_x}, \quad \mathcal{N}_y = \frac{tv_y}{L_y}, \quad \mathcal{N}_z = \frac{tg}{2v_z}, \quad (12)$$

where the vertical velocity component v_z is taken at the trap bottom $z = 0$. From Eq. (12) we already see a strong difference between the dependence of UCN collision rate on their vertical and horizontal velocities. While the collision rate with side walls is proportional to the horizontal UCN velocity and is not affected free fall acceleration, the collision rate with trap bottom is inversely proportional to the vertical UCN velocity, because there is no upper trap wall, and the neutrons fall to the bottom only because of gravity. Hence, there is a big difference between the collisions with trap bottom and side walls, which affects the usual procedure of size extrapolation of UCN loss rate to an infinitely large UCN trap.

The probability for a neutron to remain in the trap after time t is given by the product

$$P_n(t, \mathbf{v}) = P(t, \mathbf{v})e^{-t/\tau_n}, \quad (13)$$

where the probability for a neutron to be not absorbed by the trap walls is

$$P(t, \mathbf{v}) = \prod_{i=x,y,z} [1 - \mu_i(v_i)]^{\mathcal{N}_i}. \quad (14)$$

Since $\mu_i(v_i) \sim \eta \ll 1$ and $\mathcal{N}_i \sim \eta^{-1} \gg 1$, using $e = \lim_{n \rightarrow \infty} (1 + 1/n)^n$ one may simplify Eq. (14) to

$$P(t, \mathbf{v}) \approx \exp\left(-\sum_i \mathcal{N}_i \mu_i(v_i)\right) = \exp\left(-\frac{t}{\tilde{\tau}_{(e)}(\mathbf{v})}\right), \quad (15)$$

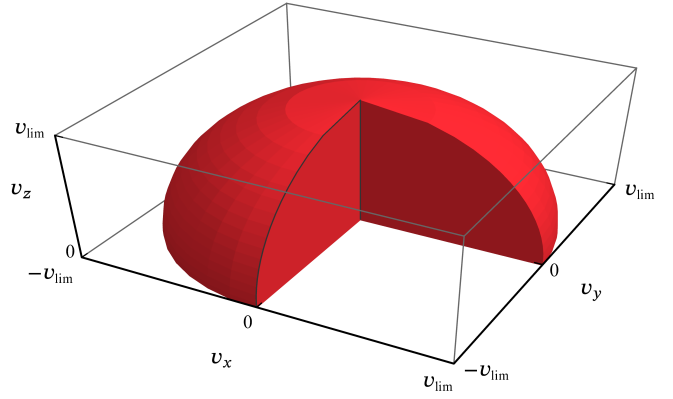


FIG. 1. Color plot of initial isotropic UCN velocity distributions. All velocities in hemisphere of radius v_{lim} are equally probable.

where the exact absorption rate

$$\tilde{\tau}_{(e)}^{-1}(\mathbf{v}) = \sum_i \frac{\mu_i(v_i)\mathcal{N}_i}{t}. \quad (16)$$

Eqs. (16) and (21) should be compared with the generally used formulas for $\tau_{(g)}^{-1}(E)$, given by Eqs. (3)–(6), and with the oversimplified formula for $\tau_{(s)}^{-1}(E)$, given by Eq. (10). The results differ because (i) the probability (15) depends not only on the velocity absolute value as in Eq. (3), but also on its direction, which is not isotropic at finite height h , and (ii) according to Eq. (12) the collision frequency with the trap bottom $\mathcal{N}_z \propto v_z^{-1}$ is inversely proportional to the normal velocity, contrary to the collision frequency with the side walls $\mathcal{N}_x \propto v_x$ and $\mathcal{N}_y \propto v_y$. Below we analytically calculate the UCN absorption rate by the walls of rectangular and cylindrical traps by these three methods and compare the results obtained.

B. Isotropic UCN velocity distribution

If the physical model described by Eq. (11) is correct, Eqs. (16) and (12) are exact for calculating the UCN absorption rate of each neutron in a rectangular trap provided its velocity \mathbf{v} at trap bottom is known. However, to use these formulas one also needs to know the UCN velocity distribution function $f_0(\mathbf{v})$ at trap bottom. Then the total UCN absorption rate

$$\tau_{(e)}^{-1} = \int d^3\mathbf{v} \tilde{\tau}_{(e)}^{-1}(\mathbf{v})f_0(\mathbf{v}). \quad (17)$$

The energy dependence of the UCN absorption rate

$$\tau_{(e)}^{-1}(E) = \int d^3\mathbf{v} \delta\left(E - \frac{m\mathbf{v}^2}{2}\right) \tilde{\tau}_{(e)}^{-1}(\mathbf{v})f_0(\mathbf{v}). \quad (18)$$

Eqs. (17) and (18) do not contain the kinematic factor $\cos\theta$ as in the calculation of collision rate (2) because this factor is already contained in the absorption rate $\tilde{\tau}_{(e)}^{-1}$.

One often assumes an isotropic and uniform *initial* velocity distribution

$$f_0(v_x, v_y, v_z) = f_0 = \text{const} \quad (19)$$

of neutrons at the trap bottom with the condition $|\mathbf{v}| \leq v_{\max}$, i.e. the uniform UCN distribution in the velocity space limited by the sphere of radius v_{\max} and volume $V_v = 4\pi v_{\max}^3/3$. This isotropic UCN velocity distribution is illustrated in Fig. 1. Usually, in UCN- τ experiments [24, 27] $v_{\max} < 0.9 v_{\text{lim}}$. The normalization condition states that the total neutron number

$$N_0 = S_b \int_{|\mathbf{v}| \leq v_{\max}} d^3\mathbf{v} f_0(v_x, v_y, v_z) = S_b f_0 \frac{4\pi}{3} v_{\max}^3, \quad (20)$$

where S_b is the area of trap bottom. For isotropic $f_0(\mathbf{v})$ the energy dependence of the UCN absorption rate is given by the integration over the solid angle:

$$\tau_{(e)}^{-1}(E) = \int \frac{d\Omega}{4\pi} \tilde{\tau}_{(e)}^{-1}(\mathbf{v}). \quad (21)$$

The isotropic velocity distribution (19) at trap bottom does not mean that at any height the UCN velocity distribution remains isotropic, because with height change the UCN vertical velocity also changes due to gravity.

One should distinguish between the total UCN *number* distribution function $f_0(\mathbf{v})$ and the *density* distribution $n(h, \mathbf{v})$ on the height h , which gives the UCN density in the 6-dimensional phase space. Below we show that the isotropic velocity distribution $f_0(\mathbf{v})$ results to anisotropic $n(h, \mathbf{v})$ and vice versa even at the trap bottom $h = 0$. If $n(h, \mathbf{v})$ is known, the UCN velocity distribution at trap bottom is given by

$$f_0(v_x, v_y, v_z) = \int_0^{h_{\max}} dh n\left(h, v_x, v_y, \sqrt{v_z^2 - 2gh}\right). \quad (22)$$

The Liouville's theorem asserts that the phase-space distribution function $\propto n(h, \mathbf{v})$ is constant along the trajectories of the system, but $n(h, \mathbf{v}) \neq \text{const}$. Moreover, a diffuse elastic UCN scattering violates the Liouville's theorem. The diffuse scattering obeying the Lambert's cosine law keeps the $n(h, \mathbf{v})$ rather than $f_0(\mathbf{v})$ isotropic, as we show in Sec. IV.

C. Limiting case of a wide trap with uniform velocity distribution at trap bottom

First, we consider a limiting case of very wide UCN trap with $L_x, L_y \gg h_{\max}$, where the neutron scattering happens only with the trap bottom at $h = 0$. We also assume isotropic and uniform velocity distribution at trap bottom, given by Eqs. (19) and (20).

1. Distribution function at arbitrary height

The distribution function $f(h, \mathbf{v})$ of neutrons on height h can be obtained from the initial uniform distribution function $f(h = 0, \mathbf{v}) = f_0(\mathbf{v}) = f_0(v_x, v_y, v_z)$ at $h = 0$ by reducing the velocity z -component as

$$v_z \rightarrow v_{zh} \equiv v_z(h) = \sqrt{v_z^2 - 2gh}, \quad v_z = \sqrt{v_{zh}^2 + 2gh} \quad (23)$$

which gives the derivatives

$$\frac{dv_{zh}}{dv_z} = \frac{v_z}{\sqrt{v_z^2 - 2gh}}, \quad \frac{dv_z}{dv_{zh}} = \frac{v_{zh}}{\sqrt{v_{zh}^2 + 2gh}}, \quad (24)$$

and the particle velocity distribution at height h

$$f(h, \mathbf{v}) \equiv f(v_x, v_y, v_{zh}) = f_0(v_x, v_y, v_z) \frac{dv_z}{dv_{zh}} \quad (25)$$

$$= f_0\left(v_x, v_y, \sqrt{v_{zh}^2 + 2gh}\right) \frac{v_{zh}}{\sqrt{v_{zh}^2 + 2gh}} = f_0 \frac{v_{zh}}{v_z}. \quad (26)$$

However, this distribution function is not proportional to neutron density distribution $n(\mathbf{v})$ on the height h or, more precisely, in the height interval $(h, h + \Delta h)$ at $\Delta h \rightarrow 0$, because the latter is also proportional to the ratio of the time

$$\Delta t(\mathbf{v}) = \Delta t(v_z, h) = \Delta h/|v_{zh}| \quad (27)$$

that each neutron spends on the height h to the total time $t_{tr} = v_z/g$ on its trajectory. Thus we obtain the particle density distribution at height h

$$n(h, \mathbf{v}) = \frac{\Delta N}{S_b \Delta h} = \frac{f(h, \mathbf{v})}{v_{zh}(v_z/g)} = \frac{f_0}{v_z^2/g} \quad (28)$$

$$= f_0\left(v_x, v_y, \sqrt{v_{zh}^2 + 2gh}\right) \frac{g}{v_{zh}^2 + 2gh}. \quad (29)$$

If $f_0(\mathbf{v}) = \text{const}$, the particle density $n(h, \mathbf{v}) \neq \text{const}$. At a large height $h \rightarrow h_{\max} = v_{\max}^2/2g$, where $2gh \gg v_{zh}^2$ and $v_{zh}^2 + 2gh \approx 2gh$, Eq. (29) gives an almost uniform and isotropic velocity distribution $n(h, \mathbf{v})$. However, at small height $h \ll h_{\max}$ we obtain an *anisotropic* velocity distribution, peaked at small $|v_{zh}|$. At $h = 0$ we have a singularity $n(h = 0, \mathbf{v}) \propto 1/v_{zh}^2 = 1/v_z^2$. In the UCN absorption rate by trap bottom this singularity of UCN density distribution at $h = 0$ cancels, because the collision rate $\mathcal{N}_c(v_z) \propto n(h = 0, \mathbf{v})v_z \approx \text{const}/v_z$, and another factor v_z comes from the absorption probability μ given by Eq. (1), as we see below.

2. Absorption rate calculated from using the particle flow on a wall

The absorption rate dN/dt by trap walls is, usually, calculated by integrating the particle flow on a wall, equal to the collision rate $\mathcal{N}_c(\mathbf{v}) = n(h, \mathbf{v})v_{\perp}$, weighted by the absorption probability $\mu(v_{\perp})$ over all UCN velocities. Here $n(h, \mathbf{v})$ is the velocity distribution of UCN density on the height h , and v_{\perp} is the velocity component perpendicular to the wall. This approach results [21, 22] to Eq. (2) and to Eq. (5) for isotropic $n(h, \mathbf{v})$. Substituting Eqs. (1) and anisotropic distribution (28) we obtain the absorption rate $dN(E_*)/dt$ by trap bottom of UCN with energy $E \leq E_*V_0$

$$\begin{aligned} \frac{dN(E_*)}{dt} &= \int_{v_z < 0} d^3\mathbf{v} n(h = 0, \mathbf{v})v_z \mu(v_z) \quad (30) \\ &= \int_{v_z < 0} d^3\mathbf{v} \frac{2f_0 g \eta / v_{\text{lim}}}{\sqrt{1 - v_z^2/v_{\text{lim}}^2}}. \end{aligned}$$

At each v_z the volume in velocity space filled by UCN is $dV = \pi(v^2 - v_z^2)dv_z$, which gives

$$\begin{aligned} \frac{dN(E_*)}{dt} &= 2\pi\eta f_0 g v_{\text{lim}}^2 \int_0^{v_*} dv_{z*} \frac{v_*^2 - v_{z*}^2}{\sqrt{1 - v_{z*}^2}} \\ &= \frac{3 N_0 \eta g / v_{\text{lim}}}{2(v_{\text{max}}/v_{\text{lim}})^3} \int_0^{\sqrt{E_*}} dx \frac{E_* - x^2}{\sqrt{1 - x^2}}, \end{aligned} \quad (31)$$

where $v_{z*} = v_z/v_{\text{lim}}$ and in the last line we used the normalization of $f_0 = N_0/(4\pi v_{\text{max}}^3/3)$. Taking the integral we obtain the UCN loss rate of neutrons with energy less than $E_* V_0$:

$$\dot{N}(E_*) = \frac{dN(E_*)}{dt} = \frac{3 N_0 \eta g / v_{\text{lim}}}{2(E_{\text{max}}/V_0)^{3/2}} f_a(E_*), \quad (32)$$

where

$$f_a(E_*) = \sqrt{E_*} \frac{\sqrt{1 - E_*}}{2} + \left(\sqrt{E_*} - \frac{1}{2} \right) \arcsin \sqrt{E_*}. \quad (33)$$

One sees that at $E_* \rightarrow 0$ this loss rate $\dot{N}(E_*) \propto E_* \rightarrow 0$:

$$f_a(E_*) \approx E_* - E_*^{3/2}/3 + E_*^2/6 + \dots, \quad E_* \rightarrow 0.$$

To calculate the total UCN loss rate one only needs to substitute $E_* = E_{\text{max}}/V_0$ to Eq. (32).

3. Alternative way of calculating the UCN absorption rate

We can also calculate the UCN absorption rate using Eq. (16). For the scattering by trap bottom we have $i = z$ and

$$\tilde{\tau}_{(e)}^{-1}(\mathbf{v}) = \sum_i \frac{\mu_i(v_i) N_i}{t} = \frac{\eta g / v_{\text{lim}}}{\sqrt{1 - v_z^2 / v_{\text{lim}}^2}}. \quad (34)$$

The total loss rate of UCN

$$\frac{dN}{dt} = -N_0 \left\langle \frac{dP(t, \mathbf{v})}{dt} \right\rangle = N_0 \left\langle \tilde{\tau}_{(e)}^{-1}(\mathbf{v}) P(t, \mathbf{v}) \right\rangle, \quad (35)$$

where the triangular brackets mean the averaging over all UCN. At $t = 0$ $P(t, \mathbf{v}) = 1$, and combining Eqs. (34) and (35) we have at $t = 0$

$$\frac{dN}{dt} = \frac{N_0}{4\pi v_{\text{max}}^3/3} \int d^3\mathbf{v} \frac{\eta g / v_{\text{lim}}}{\sqrt{1 - v_z^2 / v_{\text{lim}}^2}}. \quad (36)$$

This coincides with Eq. (30) and gives the same result. Hence, the above two methods of calculating the UCN absorption rate are equivalent provided the UCN distribution is taken the same.

D. Comparison of the absorption rate by trap bottom calculated by different methods for isotropic UCN number velocity distribution

In this subsection we again consider a very wide UCN trap with $L_x, L_y \gg h_{\text{max}}$, where the neutron scatter mainly by the

trap bottom at $h = 0$, and calculate the energy dependence of the absorption rate by three different methods. This may be useful if the energy distribution of UCN is known and differs from the one corresponding to uniform velocity distribution in Eq. (19), as in real experiments [24, 26].

Eqs. (3)–(6), which take the gravity into account but assume (i) an isotropic UCN velocity distribution at any height and (ii) contrary to Eq. (12), the similar dependence of the effective collision rate on the vertical and horizontal UCN velocity, give

$$\tau_{z(g)}^{-1}(E) = \frac{m_n g \bar{\mu}(E) v}{4 \int_0^E dh' \sqrt{1 - h'/E}} = \frac{3}{2} \tau_{z0}^{-1} \frac{f_1(E_*)}{\sqrt{E_*}}. \quad (37)$$

Here we introduced the factor $\tau_{z0}^{-1} = g\eta/v_{\text{lim}}$, which describes the UCN absorption rate by trap bottom in order of magnitude, and the function $f_1(E_*)$ is given by Eq. (4).

When the gravity effects are neglected and an isotropic velocity distribution is assumed, for the size extrapolation in τ_n measurements one often applies Eq. (10) for calculating the UCN loss rate $\tau_{(s)}^{-1}(E)$, which just gives a geometrical surface-to-volume ratio of the UCN trap. This oversimplified method neglecting the gravity seems to be completely inapplicable for the calculation of UCN loss rate due to the collisions with trap bottom, because the corresponding collision rate $\mathcal{N}_z = g/2v_z$ in Eq. (12) is determined by gravity. Nevertheless, if we take as the "trap height" V/S in Eqs. (9) and (10) the maximum UCN height in the gravitational potential $h_{\text{max}}(E)$, given by Eq. (7), then we obtain the following simple formula for the UCN absorption rate

$$\tau_{z(s)}^{-1}(E) = \tau_{z0}^{-1} \frac{f_1(E_*)}{\sqrt{E_*}}. \quad (38)$$

It differs from $\tau_{z(g)}^{-1}(E)$ only by the factor $2/3$, which came from the integral $\int_0^1 dx \sqrt{1 - x} = 2/3$ in the denominator of Eq. (37). Physically, this difference comes because Eq. (5) takes into account the dependence of UCN density on height, given by Eq. (6), which is maximal at the trap bottom and, hence, gives a larger absorption rate by the trap bottom, while Eq. (9) assumes a uniform UCN density.

The calculation using Eqs. (11), (12), (16) and (21) for an isotropic velocity distribution (19) of UCN near the trap bottom result to a different UCN absorption rate

$$\tau_{z(e)}^{-1}(E) = \tau_{z0}^{-1} \frac{\arcsin \sqrt{E_*}}{\sqrt{E_*}}. \quad (39)$$

Eqs. (37) and (39) give the same value of the UCN absorption rate at $E = 0$ but differ considerably at $E > 0$, which follows already from their Taylor expansions at $E_* = E/V_0 \ll 1$:

$$\frac{\tau_{z(g)}^{-1}}{\tau_{z0}^{-1}} \approx 1 + \frac{3}{10} E_*, \quad \frac{\tau_{z(e)}^{-1}}{\tau_{z0}^{-1}} \approx 1 + \frac{E_*}{6}. \quad (40)$$

The oversimplified result in Eq. (38) gives different both the UCN absorption rate at $E = 0$ and its asymptotics:

$$\frac{\tau_{z(s)}^{-1}}{\tau_{z0}^{-1}} \approx \frac{2}{3} + \frac{E_*}{5}. \quad (41)$$

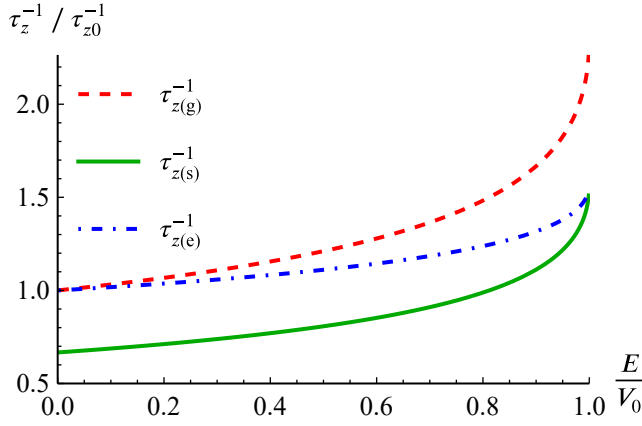


FIG. 2. The energy dependence of UCN loss rate τ_z from the absorption by trap bottom only, corresponding to a wide UCN trap. The calculations and averaging over UCN incidence angle are done in three ways: (i) the standard method, using Eqs. (3)–(6) and resulting to Eq. (37) (dashed red line), which assumes that the gravity only changes the UCN density and velocity absolute value (as a function of height) but not its angular distribution, (ii) the oversimplified method, neglecting all gravity effects and giving Eq. (38) (solid green line), and (iii) the exact calculation method for the isotropic UCN velocity distribution at trap bottom given by Eq. (19) and illustrated in Fig. 1, giving Eq. (39) (dot-dashed blue line).

The analytical results (37), (38) and (39) are plotted in Fig. 2. They hold for the UCN absorption rate by the trap bottom not only for rectangular but for any straight cylindrical trap with an arbitrary base shape.

E. Absorption by rectangular side walls

Now we consider the UCN absorption by side walls calculated using the above three methods. The standard extrapolation procedure described by Eqs. (3)–(6) for the rectangular trap of dimensions $L_x \times L_y$ gives the following UCN absorption rate by side walls

$$\tau_{r(g)}^{-1} = \frac{L_x + L_y \int_0^{h_{\max}(E)} dh \bar{\mu}(E-h')v(E-h')\rho(E,h')}{2L_x L_y \int_0^{h_{\max}(E)} dh \rho(E,h')} = 3\tau_{r0}^{-1} \frac{f_2(E_*)}{\sqrt{E_*}}, \quad (42)$$

where we introduced the factor $\tau_{r0}^{-1} = \eta v_{\text{lim}}(L_x + L_y)/2L_x L_y$ giving the UCN absorption rate by side trap walls in order of magnitude, and the dimensionless function

$$f_2(y) = \int_0^1 dx \left(\arcsin \sqrt{y(1-x)} - \sqrt{y(1-x)} \sqrt{1-y(1-x)} \right) = \left(\frac{3}{4y} - \frac{1}{2} \right) \sqrt{y(1-y)} - \left(\frac{3}{4y} - 1 \right) \arcsin \sqrt{y}. \quad (43)$$

Applying Eq. (10), which neglects gravity, we get the fol-

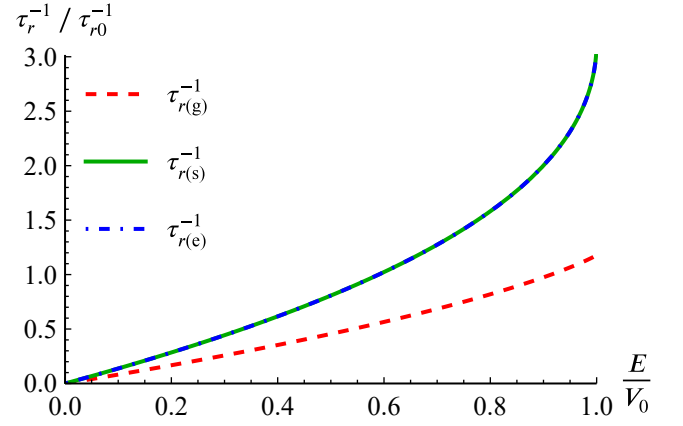


FIG. 3. The energy dependence of UCN loss rate τ_r^{-1} from the absorption by side walls only, corresponding to rectangular $L_x \times L_y$ trap, for the isotropic UCN velocity distribution at trap bottom given by Eq. (19) and illustrated in Fig. 1. The calculation is performed in three ways: the standard method, giving Eq. (42) (dashed red), the oversimplified method, giving Eq. (44) (solid green), and the proposed calculation method for a rectangular trap, giving Eq. (45) (dot-dashed blue).

lowing oversimplified absorption rate by side walls

$$\tau_{r(s)}^{-1}(E) = 2\tau_{r0}^{-1} \sqrt{E_*} f_1(E_*). \quad (44)$$

Combining Eqs. (11),(12),(16),(21) we get the absorption rate by side walls due to the UCN horizontal motion for the uniform velocity distribution (19) of UCN at trap bottom:

$$\tau_{r(e)}^{-1} = 2\tau_{r0}^{-1} \sqrt{E_*} f_1(E_*). \quad (45)$$

We see that Eqs. (45) and (44) coincide. This is not surprising because in our model the vertical and horizontal UCN motions along each main axis are separated. For a rectangular UCN trap the absorption rate by side walls depends only on the horizontal UCN velocities, which do not depend on the height h above the trap bottom, as in the oversimplified formula (10). However, as can be seen from Fig. 5 below, a similar coincidence does not hold for arbitrary UCN trap shapes, where the two horizontal UCN velocity components do not separate.

At $E_* \ll 1$ Eqs. (42) and (44) or (45) simplify to

$$\frac{\tau_{r(g)}^{-1}}{\tau_{r0}^{-1}} \simeq \frac{4}{5} E_*, \quad \frac{\tau_{r(s)}^{-1}}{\tau_{r0}^{-1}} = \frac{\tau_{r(e)}^{-1}}{\tau_{r0}^{-1}} \simeq \frac{4}{3} E_*. \quad (46)$$

These low-energy Taylor expansions differ already in the first linear-term coefficient.

In Fig. 3 we compare the UCN absorption rates by side walls given by Eqs.(42),(44) and (45). The result in Eq. (42), obtained by the standard method, differs strongly from that in Eqs. (44) and (45), as one can see already from their Taylor expansions in Eq. (46). This difference appears because the standard method (g), described by Eq. (42) and coming from Eqs. (3)–(6), assumes an isotropic UCN velocity distribution at any height. This assumption is not fulfilled for isotropic UCN velocity distribution at trap bottom given by Eq. (19)

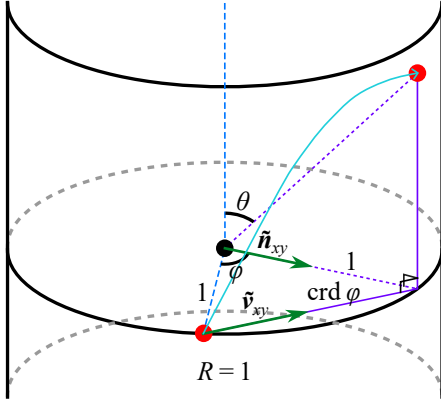


FIG. 4. Neutron path between the reflections from the side wall of a cylindrical trap. This scheme also illustrates the notations, used in the text and formulas.

because at large height the vertical velocity component is reduced by gravity, while the horizontal UCN velocity is not affected by the gravity. Hence, the normal-to-wall horizontal UCN velocity component, which enters Eq. (1), is larger than the one assumed in Eq. (42). Therefore, Eq. (42) gives a smaller absorption rate by side walls. This is especially important for the size extrapolation, which now depends on trap shapes. On contrary, in Eq. (45) the isotropic UCN velocity distribution is assumed only at $z = 0$, which corresponds to the averaging in Eq. (21).

F. Absorption by cylindrical side wall

The number of UCN collision with the side wall of a straight vertical cylinder of radius R during a long time $t \gg R/v_{xy}$ and the corresponding absorption rate, in analogy with Eqs. (12) and (16), are given by:

$$\mathcal{N}_c = \frac{tv \sin \theta}{R \text{crd} \varphi}, \quad \tilde{\tau}_{c(e)}^{-1}(\mathbf{v}) = \frac{\mu(v_{\perp}) \mathcal{N}_c}{t}, \quad (47)$$

where $\text{crd} \varphi = 2 \sin(\varphi/2)$ is the chord length in a unit circle, and $v \sin \theta$ is the neutron speed in xy plane (see Fig. 4). The neutron velocity component normal to the cylinder walls is expressed as

$$v_{\perp} = v \sin \theta (\tilde{\mathbf{v}}_{xy} \cdot \tilde{\mathbf{n}}_{xy}) = v \sin(\varphi/2) \sin \theta, \quad (48)$$

where $\tilde{\mathbf{v}}_{xy} = (\cos \varphi - 1, \sin \varphi) / \text{crd} \varphi$ is the unit direction vector of UCN velocity in the xy -plane, $\tilde{\mathbf{n}} = (\cos \varphi, \sin \varphi)$ is the unit vector normal to circle in the xy -plane at the intersection point.

Averaging Eq. (47) over angles, we get the absorption rate

$$\tau_{c(e)}^{-1} = \tau_{c0}^{-1} \sqrt{E_*} \left(\arcsin \sqrt{E_*} + \frac{f_1(E_*)}{2} \right), \quad (49)$$

where we introduced $\tau_{c0}^{-1} = \eta v_{\text{lim}} / 2R$ describing the UCN absorption rate by cylindrical side wall in the order of magnitude.

The standard calculation method described by Eqs. (3)-(5) for the cylindrical trap of radius R gives the side-wall

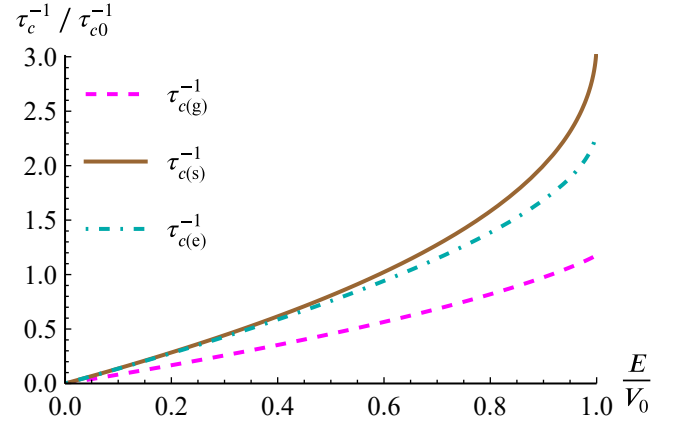


FIG. 5. The energy dependence of UCN loss rate τ_c^{-1} from the absorption by side wall of a straight cylindrical trap of radius R for the isotropic UCN velocity distribution at trap bottom given by Eq. (19) and illustrated in Fig. 1. The calculation and averaging over the UCN incidence angle is performed in three ways: the standard method, giving Eq. (50) and shown by dashed magenta line, the oversimplified method, resulting to Eq. (51) (solid brown line), and the proposed calculation method for a cylindrical trap, giving Eq. (49) (dot-dashed cyan line).

absorption rate

$$\tau_{c(g)}^{-1}(E) = 3\tau_{c0}^{-1} \frac{f_2(E_*)}{\sqrt{E_*}}. \quad (50)$$

It resembles the expression (42) derived for the rectangular trap except for the coefficient $\tau_{r0}^{-1} \rightarrow \tau_{c0}^{-1}$.

The oversimplifies method neglecting the gravity and described by Eq. (10) gives

$$\tau_{c(s)}^{-1}(E) = 2\tau_{c0}^{-1} \sqrt{E_*} f_1(E_*). \quad (51)$$

The results given by Eqs. (51) and (49) differ, which follows from the quadratic term of their Taylor expansions at $E_* \ll 1$:

$$\frac{\tau_{c(s)}^{-1}}{\tau_{c0}^{-1}} \simeq \frac{4}{3}E_* + \frac{2}{5}E_*^2, \quad \frac{\tau_{c(e)}^{-1}}{\tau_{c0}^{-1}} \simeq \frac{4}{3}E_* + \frac{4}{15}E_*^2. \quad (52)$$

Eq. (50), corresponding to the standard calculation method, differs from two other methods much stronger, already in the linear order:

$$\frac{\tau_{c(g)}^{-1}}{\tau_{c0}^{-1}} \simeq \frac{4}{5}E_*. \quad (53)$$

In Fig. 5 we compare the UCN absorption rates by cylindrical side walls calculated by all three methods and given by Eqs. (49),(50) and (51). We see that the results of proposed and oversimplified methods, given by Eqs. (49) and (51) correspondingly, now differ but not strongly, mainly at large neutron energy approaching the potential barrier height V_0 . On contrary, the UCN loss rates calculated by the standard method and given by Eq. (50) is very different. This difference is similar to the case of rectangular side walls, considered in Sec. III E and illustrated in Fig. 3, and have the same origin, discussed in the end of Sec. III E.

G. Total absorption rate and size extrapolation

From Figs. 2, 3, and 5 we see that the UCN absorption rate and its dependence on UCN energy differ strongly for trap bottom and side walls. This means that the UCN absorption rate changes differently if the trap dimensions are reduced along the vertical z or horizontal x, y axes. This is very important because it affects the procedure of size extrapolation, on which all current precise τ_n UCN storage measurements are based to account for the difference $\gtrsim 2\%$ between the measured and extracted neutron lifetime. Our calculations show that the result of the size extrapolation depends strongly on the shapes of large and reduced UCN traps, i.e. on the position and shape of the trap insert in UCN- τ experiments.

To illustrate this message and to estimate possible error in the estimates of neutron loss rate we now compare the UCN absorption rate calculated using the above three methods for a rectangular (cylindrical) UCN trap of typical dimensions $L_x, L_y \sim h_{\text{lim}}$ for rectangular and $R \sim h_{\text{lim}}$ for cylindrical traps. Evidently, the total absorption rate τ^{-1} is given by the sum of the absorption rate τ_z^{-1} by trap bottom due to the vertical UCN motion and the absorption rate τ_r^{-1} (τ_c^{-1}) by side walls due to the horizontal UCN velocity.

For the rectangular trap the total absorption rate

$$\tau_R^{-1}(E_*) = \tau_z^{-1}(E_*) + \tau_r^{-1}(E_*). \quad (54)$$

It is convenient to introduce the dimensionless parameter $h_* = h_{\text{lim}}(L_x + L_y)/2L_xL_y = h_{\text{lim}}(L_x^{-1} + L_y^{-1})/2$, which describes the UCN trap size and enters all the expressions for absorption rate. At $L_x = L_y = L$ this size parameter $h_* = h_{\text{lim}}/L$, and $\tau_{r0}^{-1} = 2\tau_{z0}^{-1}h_*$. Combining Eqs. (54), (38) and (44) we obtain for the oversimplified method without gravity the following total UCN absorption rate:

$$\tau_{R(s)}^{-1}(E_*) = \tau_{z0}^{-1} \frac{f_1(E_*)}{\sqrt{E_*}} (1 + 4h_*E_*). \quad (55)$$

Combining Eqs. (54), (37) and (42) gives the result of standard method where the gravity changes only the UCN energy and concentration as a function of height:

$$\tau_{R(g)}^{-1}(E_*) = \frac{3}{2}\tau_{z0}^{-1} \frac{f_1(E_*)}{\sqrt{E_*}} \left(1 + 4h_* \frac{f_2(E_*)}{f_1(E_*)}\right). \quad (56)$$

Eqs. (54), (39) and (45), derived exactly for the isotropic velocity distribution (19) at trap bottom, give the following total UCN absorption rate by the walls of rectangular trap:

$$\tau_{R(e)}^{-1}(E_*) = \tau_{z0}^{-1} \frac{f_1(E_*)}{\sqrt{E_*}} \left(\frac{\arcsin \sqrt{E_*}}{f_1(E_*)} + 4h_*E_* \right). \quad (57)$$

Let us compare a rectangular trap with a cylindrical one at the same volume to height ratio, i.e. the same base area $V/h_{\text{lim}} = L^2 = \pi R^2$. Then $h_* = h_{\text{lim}}/(R\sqrt{\pi})$ and $\tau_{c0}^{-1} = \sqrt{\pi}\tau_{z0}^{-1}h_*$. Performing the same steps as for a rectangular trap, but using

$$\tau_C^{-1}(E_*) = \tau_z^{-1}(E_*) + \tau_c^{-1}(E_*) \quad (58)$$

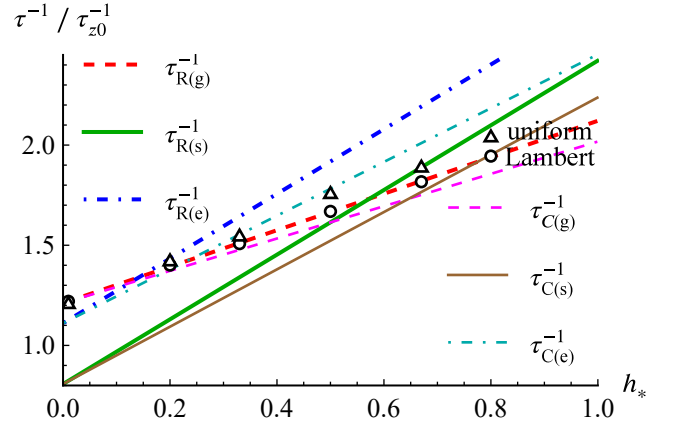


FIG. 6. The dependence of UCN loss rate τ^{-1} on the reduced inverse trap size h_* at $E_* = 1/2$ for the isotropic UCN velocity distribution at trap bottom given by Eq. (19) and illustrated in Fig. 1. Rectangular and cylindrical traps are taken with equal areas, so that $L = R\sqrt{\pi}$. The averaging over the UCN incidence angle is performed in three ways: (i) the standard method, resulting to Eqs. (56) and (60) and illustrated by dashed lines (the red line corresponds to rectangular trap and the magenta line corresponds to cylindrical trap), function of height but not its angular distribution, (ii) the oversimplified method, neglecting all gravity effects and giving Eqs. (55) and (59) (green and brown solid lines), and (iii) the enhanced calculation method resulting to Eqs. (57) and (61), shown by the blue and cyan dot-dashed lines. The circle and triangle symbols give the results of our Monte-Carlo simulations in rectangular traps of the same dimensions including the diffuse UCN scattering by the trap walls with probability $p_d = 0.1$ and obeying the Lambert's law (circles) and uniform distribution (triangles) of diffusively scattered neutrons, as discussed in Sec. IV.

instead of Eq. (54), we get the analytical formulas for the total UCN absorption rate in a cylindrical trap for all three methods. Combining Eqs. (58), (38) and (51) we obtain the oversimplified result

$$\tau_{C(s)}^{-1}(E_*) = \tau_{z0}^{-1} \frac{f_1(E_*)}{\sqrt{E_*}} (1 + 2\sqrt{\pi}h_*E_*), \quad (59)$$

Combining Eqs. (58), (37) and (50) gives the standard-method estimate of UCN absorption rate

$$\tau_{C(g)}^{-1}(E_*) = \frac{3}{2}\tau_{z0}^{-1} \frac{f_1(E_*)}{\sqrt{E_*}} \left(1 + 2\sqrt{\pi}h_* \frac{f_2(E_*)}{f_1(E_*)}\right), \quad (60)$$

Eqs. (58), (39) and (49), based on Eqs. (16)-(19), give

$$\tau_{C(e)}^{-1}(E_*) = \tau_{z0}^{-1} \left[\frac{\arcsin \sqrt{E_*}}{\sqrt{E_*}} (1 + \sqrt{\pi}h_*E_*) + \frac{\sqrt{\pi}}{2} h_* \sqrt{E_*} f_1(E) \right]. \quad (61)$$

In Fig. 6 we compare the geometrical size scaling of UCN loss rates in a rectangular and cylindrical traps calculated by three different methods for a typical UCN energy $E = V_0/2$. The green and brown solid lines show the oversimplified result

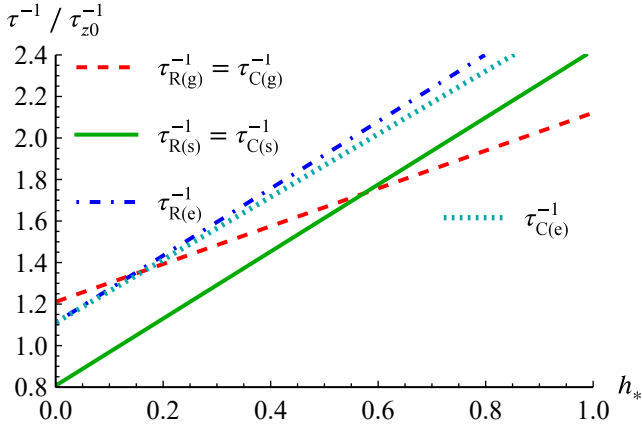


FIG. 7. The dependence of UCN loss rate τ^{-1} on the reduced inverse trap size h_* at $E_* = 1/2$. The difference from Fig. 6 is that here the comparison is at $L = 2R$.

in Eqs. (55) and (59) for rectangular and cylindrical traps correspondingly, where the gravity effects are neglected and the isotropic velocity distribution of UCN is assumed. The red and magenta dashed lines illustrate the improved approximate formulas (5) and (3), applied in Refs. [24, 27] and resulting to Eqs. (56) and (60), where the gravity effect is included via the height-dependent UCN energy and concentration, but the isotropic velocity distribution of UCN is assumed at any height and the collision rate with trap bottom is proportional to UCN vertical velocity. The dot-dashed blue and cyan lines show the UCN absorption rates by rectangular and cylindrical trap walls given by Eqs. (57) and (61), calculated exactly for the isotropic velocity distribution (19) of UCN at trap bottom.

As one can see from Fig. 6 or from Eqs. (56)-(61), the absorption rate τ^{-1} depends linearly on h_* . All three calculation methods give very different values $\tau^{-1}(h_* = 0)$, corresponding to the absorption rate by trap bottom only and describing a very wide UCN trap. This difference exceeds 10% even for the improved approximate method including gravity, which may result to the error up to ~ 2 seconds in the estimate of neutron lifetime τ_n . Hence, the size extrapolation by changing the trap base area gives very different UCN absorption rates for the considered three methods.

The linear $\tau^{-1}(h_*)$ dependence and the same value $\tau^{-1}(h_* = 0)$ for the rectangular and cylindrical traps calculated by the same method can be used to scale the plots in Fig. 6 by changing the definition of h_* for the cylindrical trap from $h_* = h_{\text{lim}}/(R\sqrt{\pi})$ to $h_* = h_{\text{lim}}/(2R)$, corresponding to $L = 2R$ and $\tau_{z0}^{-1} = 2\tau_{z0}^{-1}h_*$. In this case, the standard (g) and oversimplified (s) formulas for cylindrical trap coincide exactly with those obtained for a rectangular trap and given by Eqs. (56), (55). This is illustrated in Fig. 7. Only the isotropic UCN velocity distribution (19), resulting to Eqs. (57) and (61), gives

$$\tau_{C(e)}^{-1}(E_*) = \tau_{z0}^{-1} \left[\frac{\arcsin \sqrt{E_*}}{\sqrt{E_*}} (1 + 2h_*E) + h_*\sqrt{E_*}f_1(E) \right], \quad (62)$$

i.e. slightly different results for cylindrical and rectangular traps with the deviation less than 4%, see Fig. 7, because it

explicitly takes into account the specular reflection of neutrons from the cylindrical walls.

IV. MONTE-CARLO SIMULATION AND THE ROLE OF DIFFUSE SCATTERING

Before we considered only the specular UCN reflection from the trap walls. However, there is a small probability $p_d \lesssim 0.1$ of a diffuse UCN reflection by an arbitrary angle, which conserves only the absolute value of UCN velocity and its energy. This elastic diffuse reflection is much more probable than the UCN inelastic scattering or absorption, $p_d \gg \eta$, and must be considered. The rare diffuse scatterings mean that the UCN velocity direction in Eq. (15) after many reflections may becomes arbitrary. As we show below, the diffuse scattering changes the uniform and isotropic number distribution function (19) of UCN velocity at trap bottom, making instead the UCN density distribution $n(h, \mathbf{v})$ to be isotropic.

Usually, in Monte-Carlo simulations one takes [46–51] the Lambert's cosine law for UCN angular velocity distribution after the diffuse scattering :

$$p_L(\theta) = 2 \cos \theta, \quad (63)$$

where θ is the angle between the normal to the wall and the UCN velocity after the diffuse scattering. This distribution $p(\theta)$ is normalized:

$$\int_0^{\pi/2} d\theta p(\theta) \sin \theta = 1. \quad (64)$$

Even in optics, the Lambert's law is not universal, and there are many deviations from it [62–64]. These deviations are very important in optical spectroscopy, for example, for biological analysis [64]. For diffuse neutron scattering, there is no strict derivation of the Lambert's law at all. Small defects in the trap walls, having a characteristic size smaller than the UCN wavelength $\lambda \sim 100$ nm, give a uniform angular distribution $I(\theta) = \text{const}$ of the probability of UCN diffuse scattering, quite different from the Lambert's law (63). Such defects include surface roughness, nanopores, impurities, etc. Even ultrasmooth surfaces obtained after their multiple processing always have roughness on the submicron scale of $\lesssim 100$ nm, clearly visible with an atomic force and/or scanning electron microscope. For example, the ultrasmooth surface of nickel or beryllium intended for ultraviolet mirrors of space satellites has noticeable roughness of $\lesssim 100$ nm in size, visible with an atomic force microscope [65]. Beryllium was previously actively used for UCN traps [22, 23]. Modern UCN material traps use a coating of perfluoropolyether – Fomblin brand oil, which does not contain hydrogen [24, 27], the surface of which at the submicron scale $\lesssim 100$ nm also has strong roughness [66–68]. Large wall roughness or pores of size $d \gg \lambda$ in the material trap, which scatter with a small transmission of the wave vector $\sim 1/d$, blur the peak of specular reflection in the angular distribution of the UCN velocity after diffuse scattering and also do not give the Lambert's law. The main argument in favor of Lambert's law is the principle of detailed balance

of the UCN velocity distribution, which requires that the probability of scattering from walls is proportional to $\cos \theta$, since the collision frequency is also $\propto \cos \theta$ (see p. 96 of [22]). Neglecting gravity, the Lambert's law indeed maintains an isotropic velocity distribution and even makes an anisotropic gas more isotropic, changing the angular distribution of neutron velocities at the wall surface to their isotropic distribution. The Lambert's law provides an isotropic velocity distribution only if gravity is negligible. In the large open-top UCN material traps used in neutron lifetime measurements [24, 27], the velocity isotropy is partially provided by specular reflections from curved walls with various local surface orientations.

The microscopic calculation of the UCN diffuse scattering law is a complicated and still open problem. Recently, a simple experimental test to measure the deviations from the Lambert's cosine law for UCN diffuse scattering has been proposed [69], but such an experiment is not yet performed. For our Monte-Carlo calculations we use two limiting cases of the generalized UCN diffuse scattering law

$$p_d(\theta) = p_L 2 \cos \theta + 1 - p_L, \quad (65)$$

where p_L is the probability that the diffuse scattering obeys the Lambert's cosine law, and $1 - p_L$ that it obeys the isotropic diffuse reflection. Evidently, this angular distribution (65) also satisfies the normalization condition (64).

The results of our Monte-Carlo calculations of the UCN absorption rate in rectangular UCN traps of various bottom area for the Lambert's cosine law, $p_L = 1$, and for isotropic law, $p_L = 0$, of diffuse neutron scattering by trap walls are shown in Fig. 6 by open circles and triangles correspondingly. The calculations with Lambert's diffuse scattering confirm the result (g) given by Eq. (56), obtained using the standard method described by Eq. (5). On contrary, the result (e) in Eq. (57), obtained assuming the uniform UCN distribution (19), is not confirmed by our Monte-Carlo calculations. Let us understand the physical reason of these results.

If the diffuse scattering kept the overall isotropic velocity distribution (19), one could use Eqs. (21) with the absorption rate given by the exact Eq. (16). This would confirm the analytical results (e) obtained in Sec. III. However, this simple approach does not work because the diffuse scattering violates the uniform velocity distribution (19). Instead, as expected from the principle of detailed balance of the UCN velocity distribution [22], it is the UCN density near the wall rather than the UCN number that has the uniform velocity distribution due to the Lambert's diffuse scattering, as we illustrate below by our Monte-Carlo calculations.

In Fig. 8 we plot the v_x - v_z velocity distribution of neutron density on the height $h = 0.5h_{\max}$ (left column), $h = 0.1$ m (center column) and $h = 0.01$ m (right column) in a rectangular trap with 1×1 m² bottom size for the Lambert's law of diffuse scattering with probability $p_d = 0.1$ (upper row), $p_d = 0.0001$ (middle row), and $p_d = 0$ (lowest row). The circle radius of UCN velocity distribution is reduced with height because the UCN kinetic energy and velocity absolute value decrease with height. From Fig. 8 we see that even for a very small probability $p_d = 0.0001$ of diffuse scattering (middle row) obeying the Lambert's law the velocity distribution of

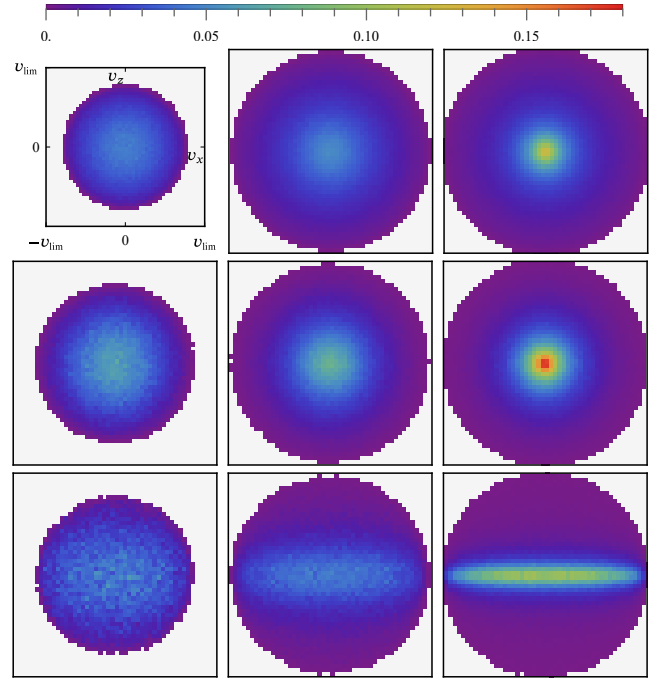


FIG. 8. Slices of neutron probability (density) distribution (PDF) $n(v_x, v_z)$ at height $h = 0.5$ m (left column), $h = 0.1$ m (center column) and $h = 0.01$ m (right column) in a trap with 1×1 m² bottom size. Probability of diffuse (Lambertian) scattering $p_d = p_L = 0.1, 0.0001$ and 0 from top to bottom. Data for averaging the PDF are collected within a 1000 s time interval after the thermodynamic equilibrium has been established. The time to establish equilibrium is estimated as $\tau_{\text{eq}} \approx 10L/(p_d v_{\text{lim}})$, where $L = \sqrt[3]{L_x L_y h_{\text{lim}}}$. In the case of $p_d = 0$ the equilibrium is never achieved, so there is no point to wait for it and we set $\tau_{\text{eq}} = 0$. Angular velocity distribution of UCN density is always isotropic and $n(\theta) = \sin(\theta)/2$ for $p_d \neq 0$.

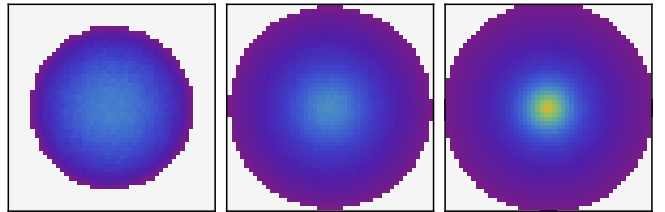


FIG. 9. Same as top row of Fig. 8 with $p_d = 0.1$ and $p_L = 1$, but bottom size is 10000×10000 m². The distribution did not change with increasing trap size.

UCN density becomes isotropic at any height after some time exceeding $\tau_{\text{eq}} \approx 10L/(p_d v_{\text{lim}})$ – the time when UCNs reach an equilibrium distribution. This isotropy is somehow expected [22] because the Lambert's law keeps the detailed balance of the UCN velocity distribution. The surprising fact is that this isotropy appears at any height when the diffuse scattering is included. This equilibrium isotropic velocity distribution of UCN density at any height is not only a consequence of the side-wall diffuse scattering but appears even if the scattering by trap bottom is dominating. To show this fact, in Fig. 9 we plot the velocity distribution of UCN density for $p_d = 0.1$

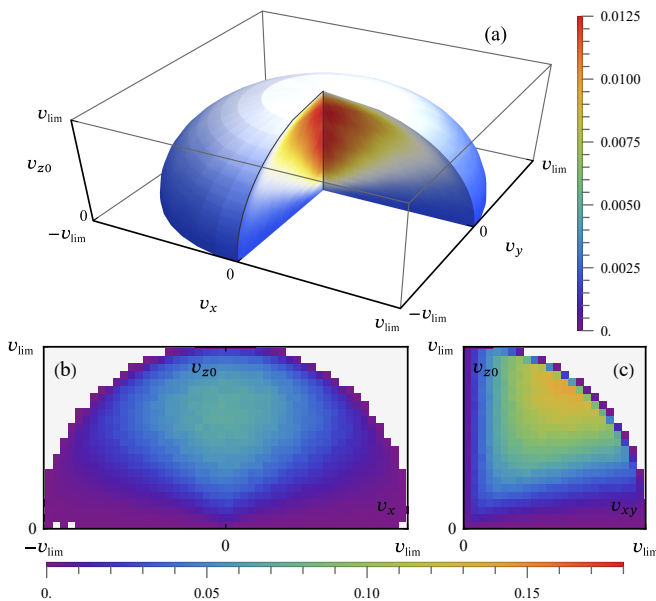


FIG. 10. (a) Slice of neutron PDF $n(v_x, x_y, v_{z0})$, where $v_{z0} = \sqrt{v_z^2 + 2gz}$ is the vertical speed of a neutron that it has when reaches the trap bottom in the Earth gravity potential. (b,c) Neutron PDFs $n(v_x, v_{z0})$ and $n(v_{xy}, v_{z0})$, where $v_{xy} = \sqrt{v_x^2 + v_y^2}$. The snapshot of the distribution was taken at the end of the Monte Carlo simulation, long after thermodynamic equilibrium had been reached. One can check numerically that these plots correspond to the distribution by azimuth angle $n(\theta_0) = 3/2 \sin^3(2\theta_0) \cos(\theta_0)$, where $\theta_0 = \arccos(v_{z0}/v_0)$. Entering polar coordinates in the v_x - v_{z0} plane with polar angle $\alpha = \text{atan2}(v_{z0}, v_x) = \arctan(v_{z0}/v_x)$ one can also numerically check that the distribution by this angle is given by $n(\alpha) = (7/11) \sin^2 \alpha$. This distribution is symmetric with respect to $\alpha = \pi/2$, which is clear from panel (b).

and $p_L = 1$ in a very wide trap $10000 \times 10000 \text{ m}^2$ where the neutrons scatter mainly by trap bottom.

As we explicitly calculated in Sec. III C 1, the isotropic velocity distribution of UCN density, obtained in our Monte-Carlo simulations and illustrated in Figs. 8 and 9, means anisotropic velocity distribution of UCN total number, and vice versa. In Fig. 10 we show the 3D color plot of UCN number velocity distribution at the trap bottom with the Lambert's law of diffuse scattering with $p_d = 0.1$. We see that it differ strongly from the original uniform velocity distribution shown in Fig. 1. This means that the uniform velocity distribution (19) does not hold with the diffuse scattering by trap walls even if the probability of this diffuse scattering $p_d \ll 1$. Hence, method (e), although being exact for the UCN distribution (19), does not describe well the UCN traps. On contrary, the standard method (g) assumes a different UCN velocity distribution, which is much closer to the UCN distribution at equilibrium, illustrated in Figs. 8-10. Hence, it better describes the UCN absorption rate, as one sees from the comparison shown in Fig. 6.

If the diffuse UCN scattering does not obey the Lambert's cosine law, e.g. if $p_L \neq 1$ in Eq. (65), the velocity distribution of UCN density is not isotropic in equilibrium. Then, as

we show in Fig. 6, there are considerable deviations of the UCN absorption rate from that calculated using the standard method (g) based on Eq. (5) or using the MC simulations [46–51] assuming the Lambert's diffuse scattering. Hence, the knowledge of correct velocity distribution of UCN after the diffuse scattering by trap walls is crucial for increasing the accuracy of the estimates of UCN loss rate in material traps. A microscopic theoretical model of UCN diffuse scattering by material walls is not developed yet, but a simple experimental test of the Lambert's cosine law was proposed recently [69].

We also numerically checked Eq. (6), used in the standard calculations, and found that it is valid up to the coefficient $g(E)$, which depends on the UCN energy distribution: $\rho(E, h) \propto g(E) \sqrt{(E - h')}/E$. However, this additional coefficient $g(E)$ does not affect the energy dependence of the absorption rate in Eq. (5) because it is contained both in the numerator and denominator of Eq. (5) and cancels.

V. DISCUSSION AND CONCLUSIONS

In this paper we reanalyze the standard calculation methods of UCN absorption rate by the walls of material traps, which is crucial for the accuracy of neutron lifetime measurements. The standard analytical formulas (3)–(6) take the gravity into account but assume (i) an isotropic UCN velocity distribution at any height and (ii) the similar dependence of the effective collision rate on the vertical and horizontal UCN velocity. The latter evidently contradicts Eq. (12) giving the exact collision rates for rectangular UCN traps, where the vertical and horizontal neutron motion separate. To analyze how well these approximations of the standard method are fulfilled and how they affect the estimates of neutron loss rate we calculate the UCN absorption rate by the rectangular and cylindrical trap walls without these assumptions, i.e. using Eqs. (12) and (1) for isotropic and uniform UCN velocity distribution given by Eq. (19). Then we compare the analytical results obtained by various methods with numerical Monte-Carlo calculations.

We succeeded to perform analytical calculations for UCN absorption rates in UCN traps of simple rectangular and cylinder shape in three different models: (1) the oversimplified method, neglecting gravity at all and based on Eqs. (9) and (10); (2) the improved formulas (3)–(6), applied in Refs. [24, 27] as a standard method, where the gravity effect is included via the height-dependent UCN energy and concentration only; (3) by a direct calculation using Eqs. (1),(12) and (16), which give Eq.(21) for the uniform UCN velocity distribution (19) illustrated in Fig. 1.

Our results of Sec. III, illustrated in Figs. 2-7, give several observations. First, the UCN absorption rates calculated by these three methods differ considerably, by $\geq 10\%$, both for rectangular and cylindrical traps. It is important because may give an error up to few seconds in the extracted neutron lifetime τ_n . Second, the results of size extrapolation depend strongly on the trap shape and, hence, must be done with a great care. The size scaling and extrapolation to an infinite trap is a standard and necessary procedure for extracting τ_n . We have shown that the change of trap dimensions along the

vertical and horizontal directions affects the UCN loss rate τ^{-1} differently. Hence, the results of size extrapolation in UCN- τ experiments depend on the shape and size of both trap and its insert. Third, in a gravity potential there is a strong difference between the velocity distribution of particle number and of particle density. The method (g) described by Eq. (5) corresponds to the isotropic velocity distribution of UCN density, while the method (e) corresponds to the isotropic and uniform velocity distribution of UCN number at trap bottom given by Eq. (19). Forth, we obtain explicit analytical formulas for the UCN absorption rates in the material traps of simplest geometry, rectangular and cylindrical, by both methods (g) and (e), as well as by the oversimplified method (s) neglecting gravity.

Our numerical Monte-Carlo calculations in Sec. IV also give several important results. First, they show that with UCN diffuse scattering by trap walls according to the Lambert's cosine law the UCN absorption rate is quite accurately described by the analytical formulas corresponding to the standard method (g), given by Eq. (5) and used in Refs. [24, 27], as illustrated in Fig. 6. This result means that the diffuse scattering makes the UCN density rather than the UCN number at trap bottom to have an isotropic velocity distribution. This conclusion is directly confirmed by our Monte-Carlo calculations, as illustrated in Figs. 8-10. Second, the UCN absorption rate depends considerably on the law of diffuse neutron scattering by material walls, as illustrated in Fig. 6. For an isotropic diffuse neutron scattering by trap walls the UCN velocity distribution differs essentially from that for Lambert's cosine law (compare the open triangles and circles in Fig. 6). Hence, any deviations from the Lambert's cosine law of diffuse UCN scattering may considerably affect the estimates of UCN losses in material traps and the accuracy of neutron lifetime extracted from the measurements. These deviations may be partially responsible for the four-second difference between the UCN- τ measurements using material [27] and magnetic [3] traps.

A possible way to increase the accuracy of UCN loss-rate estimates is to use the Monte-Carlo simulations [46–51], where the trajectory of each neutron is calculated with allowance for gravity. These simulations also confirm [27, 46, 47, 49, 50] the standard method of UCN loss calculation given by formulas (3)–(6) and used to analyze the experimental data in Refs. [24, 27]. This method and the corresponding our analytical formulas are marked by symbol (g). However, the

physical model used in these numerical calculations requires some clarification. In the Monte-Carlo simulations, usually, the Lambert's cosine law of the angular dependence of UCN diffuse scattering intensity is applied [46–51]. In Sec. IV, between Eqs. (64) and (65), we argue that the Lambert's law may not hold for the diffuse UCN scattering and requires an experimental test, e.g., as proposed in Ref. [69]. The angular distribution of UCN velocity after the diffuse scattering by a real trap wall is an interesting fundamental problem, which is beyond the scope of this paper. However, the estimates of UCN loss probability and the corresponding accuracy of τ_n -measurements depend strongly on this issue, as we illustrated in Fig. 6 using our Monte-Carlo simulations.

To summarize, we discuss the approximations and possible errors of the standard calculations of neutron loss rate due to the absorption by trap walls, which are very important for the precise measurements of neutron lifetime and, possibly, of its electric dipole moment. To illustrate the effect of these approximations we calculate analytically and numerically the neutron absorption rate by the walls of rectangular and cylindrical UCN traps using different methods. Our results show that the standard calculation method of UCN absorption rate, given by Eq. (5) and used in Ref. [27], is quite precise if the Lambert's cosine law of neutron scattering by material walls holds. However, this method of calculation of UCN losses, as well as the numerous Monte-Carlo calculations [27, 46, 47, 49, 50] based on the Lambert's cosine law of diffuse neutron scattering by trap walls, may give a considerable errors when there are deviations from the Lambert's cosine law of diffuse UCN scattering by real material walls. This may partially explain a four-second discrepancy between the results of recent precise neutron lifetime measurements in magnetic [36] and material [27] UCN traps. The Monte-Carlo simulations may help to estimate UCN losses quite accurately, but a physical model of diffuse neutron scattering by trap walls must be elaborated to raise more the precision and reliability of these simulations.

VI. ACKNOWLEDGMENTS

The work of V.D.K. and P.D.G. is supported by the Russian Science Foundation grant # 23-22-00312.

-
- [1] D. Dubbers and M. G. Schmidt, *Rev. Mod. Phys.* **83**, 1111 (2011).
 - [2] H. Abele, *Progress in Particle and Nuclear Physics* **60**, 1 (2008).
 - [3] M. Gonzalez-Alonso, O. Naviliat-Cuncic, and N. Severijns, *Progress in Particle and Nuclear Physics* **104**, 165 (2019).
 - [4] M. Gorchtein and C.-Y. Seng, *Universe* **9**, 422 (2023).
 - [5] M. J. Ramsey-Musolf and S. Su, *Physics Reports* **456**, 1 (2008).
 - [6] F. E. Wietfeldt and G. L. Greene, *Rev. Mod. Phys.* **83**, 1173 (2011).
 - [7] H. Abele, A. Alekou, A. Algora, K. Andersen, S. Baessler, L. Barron-Palos, J. Barrow, E. Baussan, P. Bentley, Z. Berezhi-ani, Y. Bessler, A. Bhattacharyya, A. Bianchi, J. Bijnsens,

- C. Blanco, N. B. Kraljevic, M. Blennow, K. Bodek, M. Bogomilov, C. Bohm, B. Bolling, E. Bouquerel, G. Brooijmans, L. Broussard, O. Buchan, A. Burgman, H. Calen, C. Carlile, J. Cederkall, E. Chanel, P. Christiansen, V. Cirigliano, J. Collar, M. Collins, C. Crawford, E. C. Morales, P. Cupial, L. D'Alessi, J. M. Damian, H. Danared, D. Dancila, J. de Andre, J. Delahaye, S. Degenkolb, D. Di Julio, M. Dracos, K. Dunne, I. Efthymiopoulos, T. Ekelöf, L. Eklund, M. Eshraqi, I. Esteban, G. Fanourakis, A. Farricker, E. Fernandez-Martinez, M. Ferreira, M. Fertl, P. Fierlinger, B. Folsom, A. Frank, A. Fratangelo, U. Friman-Gayer, T. Fukuda, H. Fynbo, A. G. Sosa, N. Gazis, B. Galnander, T. Gerasis, M. Ghosh, G. Gok-

- bulut, J. Gomez-Cadenas, M. Gonzalez-Alonso, F. Gonzalez, L. Halic, C. Happe, P. Heil, A. Heinz, H. Herde, M. Holl, T. Jenke, M. Jentsen, E. Jericha, H. Johansson, R. Johansson, T. Johansson, Y. Kamyshev, A. K. Topaksu, B. Kildetoft, K. Kirch, B. Kliček, E. Klinkby, R. Kolevator, G. Konrad, M. Koziol, K. Krhac, A. Kupsc, L. Lacny, L. Larizgoitia, C. Lewis, M. Lindroos, E. Lychagin, E. Lytken, C. Maiano, P. Marciniowski, G. Markaj, B. Markisch, C. Marrelli, C. Martins, B. Meirose, M. Mezzetto, N. Milas, D. Milstead, F. Monrabal, G. Muhrer, A. Nepomuceno, V. Nesvizhevsky, T. Nilsson, P. Novella, M. Oglakci, T. Ohlsson, M. Ovegard, A. Oskarsson, T. Ota, J. Park, D. Patrzalek, H. Perrey, M. Persoz, G. Petkov, F. Piegsa, C. Pistillo, P. Poussot, P. Privitera, B. Rataj, D. Ries, N. Rizzi, S. Rosauero-Alcaraz, D. Rozpedzik, D. Saiang, V. Santoro, U. Schmidt, H. Schober, I. Schulthess, S. Silverstein, A. Simon, H. Sina, J. Snamina, W. Snow, T. Soldner, G. Stavropoulos, M. Stipcevic, B. Szybinski, A. Takibayev, Z. Tang, R. Tarkeshian, C. Theroine, J. Thorne, F. Terranova, J. Thomas, T. Tolba, P. Torres-Sanchez, E. Trachanas, R. Tsenov, U. Uggerhoj, G. Vankova-Kirilova, N. Vassilopoulos, R. Wagner, X. Wang, E. Wildner, M. Wolke, J. Wurtz, S. Yiu, S. Yoon, A. Young, L. Zanini, J. Zejma, D. Zerzion, O. Zimmer, O. Zormpa, and Y. Zou, *Physics Reports* **1023**, 1 (2023), particle Physics at the European Spallation Source.
- [8] G. J. Mathews, T. Kajino, and T. Shima, *Phys. Rev. D* **71**, 021302 (2005).
- [9] B. Märkisch, H. Mest, H. Saul, X. Wang, H. Abele, D. Dubbers, M. Klopff, A. Petoukhov, C. Roick, T. Soldner, and D. Werder, *Phys. Rev. Lett.* **122**, 242501 (2019).
- [10] M. Beck, W. Heil, C. Schmidt, S. Baeßler, F. Glück, G. Konrad, and U. Schmidt, *Phys. Rev. Lett.* **132**, 102501 (2024).
- [11] J. Liu, M. P. Mendenhall, A. T. Holley, H. O. Back, T. J. Bowles, L. J. Broussard, R. Carr, S. Clayton, S. Currie, B. W. Filippone, A. García, P. Geltenbort, K. P. Hickerson, J. Hoagland, G. E. Hogan, B. Hona, T. M. Ito, C.-Y. Liu, M. Makela, R. R. Mammei, J. W. Martin, D. Melconian, C. L. Morris, R. W. Pattie, A. Pérez Galván, M. L. Pitt, B. Plaster, J. C. Ramsey, R. Rios, R. Russell, A. Saunders, S. J. Seestrom, W. E. Sondheim, E. Tatar, R. B. Vogelaar, B. VornDick, C. Wrede, H. Yan, and A. R. Young (UCNA Collaboration), *Phys. Rev. Lett.* **105**, 181803 (2010).
- [12] X. Sun, E. Adamek, B. Allgeier, Y. Bagdasarova, D. B. Berguno, M. Blatnik, T. J. Bowles, L. J. Broussard, M. A.-P. Brown, R. Carr, S. Clayton, C. Cude-Woods, S. Currie, E. B. Dees, X. Ding, B. W. Filippone, A. García, P. Geltenbort, S. Hasan, K. P. Hickerson, J. Hoagland, R. Hong, A. T. Holley, T. M. Ito, A. Knecht, C.-Y. Liu, J. Liu, M. Makela, R. Mammei, J. W. Martin, D. Melconian, M. P. Mendenhall, S. D. Moore, C. L. Morris, S. Nepal, N. Nouri, R. W. Pattie, A. Pérez Gálvan, D. G. Phillips, R. Picker, M. L. Pitt, B. Plaster, D. J. Salvat, A. Saunders, E. I. Sharapov, S. Sjue, S. Slutsky, W. Sondheim, C. Swank, E. Tatar, R. B. Vogelaar, B. VornDick, Z. Wang, W. Wei, J. W. Wexler, T. Womack, C. Wrede, A. R. Young, and B. A. Zeck (UCNA Collaboration), *Phys. Rev. C* **101**, 035503 (2020).
- [13] A. N. Ivanov, M. Pitschmann, and N. I. Troitskaya, *Phys. Rev. D* **88**, 073002 (2013).
- [14] C. Abel, S. Afach, N. J. Ayres, C. A. Baker, G. Ban, G. Bison, K. Bodek, V. Bondar, M. Burghoff, E. Chanel, Z. Chowdhuri, P.-J. Chiu, B. Clement, C. B. Crawford, M. Daum, S. Emmenegger, L. Ferraris-Bouchez, M. Fertl, P. Flux, B. Franke, A. Fratangelo, P. Geltenbort, K. Green, W. C. Griffith, M. van der Grinten, Z. D. Grujić, P. G. Harris, L. Hayen, W. Heil, R. Henneck, V. H elaine, N. Hild, Z. Hodge, M. Horras, P. Iaydjiev, S. N. Ivanov, M. Kasprzak, Y. Kermaidic, K. Kirch, A. Knecht, P. Knowles, H.-C. Koch, P. A. Koss, S. Komposch, A. Kozela, A. Kraft, J. Krempel, M. Kuźniak, B. Lauss, T. Lefort, Y. Lemi ere, A. Leredde, P. Mohanmurthy, A. Mtchedlishvili, M. Musgrave, O. Naviliat-Cuncic, D. Pais, F. M. Piegsa, E. Pierre, G. Pignol, C. Plonka-Spehr, P. N. Prashanth, G. Qu em ener, M. Rawlik, D. Rebreyend, I. Rien acker, D. Ries, S. Roccia, G. Rogel, D. Rozpedzik, A. Schnabel, P. Schmidt-Wellenburg, N. Severijns, D. Shiers, R. Tavakoli Dinani, J. A. Thorne, R. Virost, J. Voigt, A. Weis, E. Wursten, G. Wyszynski, J. Zejma, J. Zenner, and G. Zsigmond, *Phys. Rev. Lett.* **124**, 081803 (2020).
- [15] M. Pospelov and A. Ritz, *Annals of Physics* **318**, 119 (2005).
- [16] C. A. Baker, D. D. Doyle, P. Geltenbort, K. Green, M. G. D. van der Grinten, P. G. Harris, P. Iaydjiev, S. N. Ivanov, D. J. R. May, J. M. Pendlebury, J. D. Richardson, D. Shiers, and K. F. Smith, *Phys. Rev. Lett.* **97**, 131801 (2006).
- [17] A. P. Serebrov, E. A. Kolomenskiy, A. N. Pirozhkov, I. A. Krasnoschekova, A. V. Vassiljev, A. O. Polushkin, M. S. Lasakov, A. K. Fomin, I. V. Shoka, V. A. Solovey, O. M. Zherebtsov, P. Geltenbort, S. N. Ivanov, O. Zimmer, E. B. Alexandrov, S. P. Dmitriev, and N. A. Dovator, *JETP Letters* **99**, 4 (2014).
- [18] V. V. Nesvizhevsky, H. G. B orner, A. K. Petukhov, H. Abele, S. Bae ler, F. J. Rue , T. St oferle, A. Westphal, A. M. Gagarski, G. A. Petrov, and A. V. Strelkov, *Nature* **415**, 297 (2002).
- [19] T. Jenke, G. Cronenberg, J. Burgd orfer, L. A. Chizhova, P. Geltenbort, A. N. Ivanov, T. Lauer, T. Lins, S. Rotter, H. Saul, U. Schmidt, and H. Abele, *Phys. Rev. Lett.* **112**, 151105 (2014).
- [20] T. Jenke, P. Geltenbort, H. Lemmel, and H. Abele, *Nature Physics* **7**, 468 (2011).
- [21] R. Golub, D. Richardson, and L. S. K., *Ultra-Cold Neutrons* (CRC Press, 1991).
- [22] V. K. Ignatovich, *The Physics of Ultracold Neutrons* (Clarendon Press, 1990).
- [23] V. K. Ignatovich, *Physics-Uspekhi* **39**, 283 (1996).
- [24] A. P. Serebrov, V. E. Varlamov, A. G. Kharitonov, A. K. Fomin, Y. N. Pokotilovski, P. Geltenbort, I. A. Krasnoschekova, M. S. Lasakov, R. R. Taldaev, A. V. Vassiljev, and O. M. Zherebtsov, *Phys. Rev. C* **78**, 035505 (2008).
- [25] S. Arzumanov, L. Bondarenko, S. Chernyavsky, P. Geltenbort, V. Morozov, V. V. Nesvizhevsky, Y. Panin, and A. Strepetov, *Physics Letters B* **745**, 79 (2015).
- [26] A. P. Serebrov, E. A. Kolomenskiy, A. K. Fomin, I. A. Krasnoschekova, A. V. Vassiljev, D. M. Prudnikov, I. V. Shoka, A. V. Chechkin, M. E. Chaikovskii, V. E. Varlamov, S. N. Ivanov, A. N. Pirozhkov, P. Geltenbort, O. Zimmer, T. Jenke, M. Van der Grinten, and M. Tucker, *JETP Letters* **106**, 623 (2017).
- [27] A. P. Serebrov, E. A. Kolomenskiy, A. K. Fomin, I. A. Krasnoschekova, A. V. Vassiljev, D. M. Prudnikov, I. V. Shoka, A. V. Chechkin, M. E. Chaikovskiy, V. E. Varlamov, S. N. Ivanov, A. N. Pirozhkov, P. Geltenbort, O. Zimmer, T. Jenke, M. Van der Grinten, and M. Tucker, *Phys. Rev. C* **97**, 055503 (2018).
- [28] Pattie, R. W., Callahan, N. B., Cude-Woods, C., Adamek, E. R., Adams, M., Barlow, D., Blatnik, M., D., Bowman, Broussard, L. J., Clayton, S., Currie, S., Dees, E. B., Ding, X., Fellers, D., Fox, W., Fries, E., Gonzalez, F., Geltenbort, P., Hickerson, K. P., Hoffbauer, M. A., Hoffman, K., Holley, A. T., Howard, D., Ito, T. M., Komives, A., Liu, C. Y., M., Makela, Medina, J., Morley, D., Morris, C. L., O'Connor, T., Penttil , S.I., Ramsey, J.C., Roberts, A., Salvat, D., Saunders, A., Seestrom, S.J., Sharapov, E.I., Sjue, S.K.L., Snow, W.M., Sprow, A., Vanderwerp, J., Vogelaar, B., P.L., Walstrom, Wang, Z., Weaver, H., Wexler, J.,

- Womack, T.L., Young, A.R., and Zeck, B.A., EPJ Web Conf. **219**, 03004 (2019).
- [29] W. Mampe, P. Ageron, C. Bates, J. M. Pendlebury, and A. Steyerl, Phys. Rev. Lett. **63**, 593 (1989).
- [30] A. Pichlmaier, V. Varlamov, K. Schreckenbach, and P. Geltenbort, Physics Letters B **693**, 221 (2010).
- [31] P. R. Huffman, C. R. Brome, J. S. Butterworth, K. J. Coakley, M. S. Dewey, S. N. Dzhosyuk, R. Golub, G. L. Greene, K. Habicht, S. K. Lamoreaux, C. E. H. Mattoni, D. N. McKinsey, F. E. Wietfeldt, and J. M. Doyle, Nature **403**, 62 (2000).
- [32] K. K. H. Leung, P. Geltenbort, S. Ivanov, F. Rosenau, and O. Zimmer, Phys. Rev. C **94**, 045502 (2016).
- [33] A. Steyerl, K. K. H. Leung, C. Kaufman, G. Müller, and S. S. Malik, Phys. Rev. C **95**, 035502 (2017).
- [34] V. F. Ezhov, A. Z. Andreev, G. Ban, B. A. Bazarov, P. Geltenbort, A. G. Glushkov, V. A. Knyazkov, N. A. Kovrizhnykh, G. B. Krygin, O. Naviliat-Cuncic, and V. L. Ryabov, JETP Letters **107**, 671 (2018).
- [35] R. W. Pattie, N. B. Callahan, C. Cude-Woods, E. R. Adamek, L. J. Broussard, S. M. Clayton, S. A. Currie, E. B. Dees, X. Ding, E. M. Engel, D. E. Fellers, W. Fox, P. Geltenbort, K. P. Hickerson, M. A. Hoffbauer, A. T. Holley, A. Komives, C.-Y. Liu, S. W. T. MacDonald, M. Makela, C. L. Morris, J. D. Ortiz, J. Ramsey, D. J. Salvat, A. Saunders, S. J. Seestrom, E. I. Sharapov, S. K. Sjue, Z. Tang, J. Vanderwerp, B. Vogelaar, P. L. Walstrom, Z. Wang, W. Wei, H. L. Weaver, J. W. Wexler, T. L. Womack, A. R. Young, and B. A. Zeck, Science **360**, 627 (2018).
- [36] F. M. Gonzalez, E. M. Fries, C. Cude-Woods, T. Bailey, M. Blatnik, L. J. Broussard, N. B. Callahan, J. H. Choi, S. M. Clayton, S. A. Currie, M. Dawid, E. B. Dees, B. W. Filippone, W. Fox, P. Geltenbort, E. George, L. Hayen, K. P. Hickerson, M. A. Hoffbauer, K. Hoffman, A. T. Holley, T. M. Ito, A. Komives, C.-Y. Liu, M. Makela, C. L. Morris, R. Musedinovic, C. O'Shaughnessy, R. W. Pattie, J. Ramsey, D. J. Salvat, A. Saunders, E. I. Sharapov, S. Slutsky, V. Su, X. Sun, C. Swank, Z. Tang, W. Uhrich, J. Vanderwerp, P. Walstrom, Z. Wang, W. Wei, and A. R. Young (UCN τ Collaboration), Phys. Rev. Lett. **127**, 162501 (2021).
- [37] J. S. Nico, M. S. Dewey, D. M. Gilliam, F. E. Wietfeldt, X. Fei, W. M. Snow, G. L. Greene, J. Pauwels, R. Eykens, A. Lamberty, J. V. Gestel, and R. D. Scott, Phys. Rev. C **71**, 055502 (2005).
- [38] A. T. Yue, M. S. Dewey, D. M. Gilliam, G. L. Greene, A. B. Laptev, J. S. Nico, W. M. Snow, and F. E. Wietfeldt, Phys. Rev. Lett. **111**, 222501 (2013).
- [39] K. Hirota, G. Ichikawa, S. Ieki, T. Ino, Y. Iwashita, M. Kitaguchi, R. Kitahara, J. Koga, K. Mishima, T. Mogi, K. Morikawa, A. Morishita, N. Nagakura, H. Oide, H. Okabe, H. Otono, Y. Seki, D. Sekiba, T. Shima, H. M. Shimizu, N. Sumi, H. Sumino, T. Tomita, H. Uehara, T. Yamada, S. Yamashita, K. Yano, M. Yokohashi, and T. Yoshioka, Prog. Theor. Exp. Phys. **2020**, 123C02 (2020).
- [40] S. Rajendran and H. Ramani, Phys. Rev. D **103**, 035014 (2021).
- [41] A. P. Serebrov, M. E. Chaikovskii, G. N. Klyushnikov, O. M. Zherebtsov, and A. V. Chechkin, Phys. Rev. D **103**, 074010 (2021).
- [42] A. P. Serebrov, Physics-Uspekhi **62**, 596 (2019).
- [43] B. Koch and F. Hummel, Phys. Rev. D **110**, 073004 (2024).
- [44] D. Dubbers, H. Saul, B. Märkisch, T. Soldner, and H. Abele, Physics Letters B **791**, 6 (2019).
- [45] E. A. Goremychkin and Y. N. Pokotilovski, JETP Letters **105**, 548 (2017).
- [46] A. K. Fomin and A. P. Serebrov, Technical Physics **68**, S424 (2023).
- [47] Fomin, Alexey and Serebrov, Anatolii, EPJ Web Conf. **219**, 03001 (2019).
- [48] N. J. Ayres, E. Chanel, B. Clement, P. G. Harris, R. Picker, G. Pignol, W. Schreyer, and G. Zsigmond, in *Proceedings of the International Conference on Neutron Optics (NOP2017)*, Vol. 22 (2018) p. 011032.
- [49] A. K. Fomin and A. P. Serebrov, Mathematical Models and Computer Simulations **10**, 741 (2018).
- [50] A. K. Fomin and A. P. Serebrov, Technical Physics **62**, 1903 (2017).
- [51] A. P. Serebrov, A. K. Fomin, A. G. Kharitonov, V. E. Varlamov, and A. V. Chechkin, Technical Physics **58**, 1681 (2013).
- [52] N. Callahan, C.-Y. Liu, F. Gonzalez, E. Adamek, J. D. Bowman, L. Broussard, S. M. Clayton, S. Currie, C. Cude-Woods, E. B. Dees, X. Ding, W. Fox, P. Geltenbort, K. P. Hickerson, M. A. Hoffbauer, A. T. Holley, A. Komives, S. W. T. MacDonald, M. Makela, C. L. Morris, J. D. Ortiz, R. W. Pattie, J. Ramsey, D. J. Salvat, A. Saunders, E. I. Sharapov, S. K. L. Sjue, Z. Tang, J. Vanderwerp, B. Vogelaar, P. L. Walstrom, Z. Wang, H. Weaver, W. Wei, J. Wexler, and A. R. Young, Phys. Rev. C **100**, 015501 (2019).
- [53] R. Golub, C. Jewell, P. Ageron, W. Mampe, B. Heckel, and I. Kilvington, Zeitschrift für Physik B Condensed Matter **51**, 187 (1983).
- [54] R. C. Bokun, Sov. J. Nucl. Phys. **40**, 287 (1984), <https://inis.iaea.org/search/16073419>.
- [55] V. P. Alfimenkov, V. K. Ignatovich, L. P. Mezhev-Deglin, V. I. Morozov, A. V. Strelkov, and T. M. I., Communications of Joint Institute for Nuclear Research, Dubna preprint (in Russian) **P3-2009-197** (2009), [http://www1.jinr.ru/Preprints/2009/197\(P3-2009-197\).pdf](http://www1.jinr.ru/Preprints/2009/197(P3-2009-197).pdf).
- [56] P. D. Grigoriev, O. Zimmer, A. D. Grigoriev, and T. Ziman, Phys. Rev. C **94**, 025504 (2016).
- [57] P. D. Grigoriev and A. M. Dyugaev, Phys. Rev. C **104**, 055501 (2021).
- [58] P. D. Grigoriev, A. M. Dyugaev, T. I. Mogilyuk, and A. D. Grigoriev, JETP Letters **114**, 493 (2021).
- [59] P. D. Grigoriev, A. V. Sadovnikov, V. D. Kochev, and A. M. Dyugaev, Phys. Rev. C **108**, 025501 (2023).
- [60] S. Ahmed, E. Altieri, T. Andalib, B. Bell, C. P. Bidinosti, E. Cudmore, M. Das, C. A. Davis, B. Franke, M. Gericke, P. Gampa, P. Gnyp, S. Hansen-Romu, K. Hatanaka, T. Hayamizu, B. Jamieson, D. Jones, S. Kawasaki, T. Kikawa, M. Kitaguchi, W. Klassen, A. Konaka, E. Korkmaz, F. Kuchler, M. Lang, L. Lee, T. Lindner, K. W. Madison, Y. Makida, J. Mammei, R. Mammei, J. W. Martin, R. Matsumiya, E. Miller, K. Mishima, T. Momose, T. Okamura, S. Page, R. Picker, E. Pierre, W. D. Ramsay, L. Rebenitsch, F. Rehm, W. Schreyer, H. M. Shimizu, S. Sidhu, A. Sikora, J. Smith, I. Tanihata, B. Thorsteinson, S. Vanbergen, W. T. H. van Oers, and Y. X. Watanabe (TUCAN Collaboration), Phys. Rev. C **99**, 025503 (2019).
- [61] O. Zimmer, Phys. Rev. C **93**, 035503 (2016).
- [62] T. G. Mayerhöfer, S. Pahlow, and J. Popp, ChemPhysChem **21**, 2029 (2020).
- [63] H. G. Hecht, J Res Natl Bur Stand A Phys Chem **80A**, 567 (1976).
- [64] M. Mamouei, K. Budidha, N. Baishya, M. Qassem, and P. A. Kyriacou, Scientific Reports **11**, 13734 (2021).
- [65] N. I. Chkhalo, M. S. Mikhailenko, A. E. Pestov, V. N. Polkovnikov, M. V. Zorina, S. Y. Zuev, D. S. Kazakov, A. V. Milkov, I. L. Strulya, V. A. Filichkina, and A. S. Kozlov, Appl. Opt. **58**, 3652 (2019).
- [66] J. M. Russell-Tanner, S. Takayama, A. Sugimura, J. M. DeSimone, and E. T. Samulski, The Journal of Chemical Physics

- 126**, 244706 (2007).
- [67] V. A. Ganesh, S. S. Dinachali, S. Jayaraman, R. Sridhar, H. K. Raut, A. Góra, A. Baji, A. S. Nair, and S. Ramakrishna, *RSC Adv.* **4**, 55263 (2014).
- [68] C. Masciullo, A. Sonato, F. Romanato, and M. Cecchini, *Nanomaterials* **8**, 609 (2018).
- [69] P. D. Grigoriev, V. D. Kochev, V. A. Tsyplyukhin, A. M. Dyugaev, and I. Y. Polishchuk, *JETP Lett.* **120**, 911 (2024), arXiv:2412.05106 [physics.ins-det].